[redacted]

IDENTIFICATION	REVISION
FS1-0015328	2.0

AREVA Front End BG
Fuel BU

AREVA

TOTAL NUMBER OF PAGES: 88

Structural Analyses of the AREVA Atrium-11 LTA Fuel Assembly in the RAJ-II Container during Normal and Accident Transport Conditions

ADDITIONAL INFORMATION:

Status Code: Approved
Document Supplier: ATKINS Nuclear Solutions US.
AREVA Purchase Order: Purchase Authorization 83 9241222 000 of 2 June 2015
Suppler Report Number: NSA DAC AREVA 14 01 Rev 1; "Structural Analyses of the AREVA Atrium 11 LTA Fuel Assembly in the RAJ II Container during Normal and Accident Transport Conditions"
Cold STOR: No

PROJECT	
HANDLING	[redacted]
CATEGORY	CLD - Client Document
STATUS	

DISTRIBUTION TO	PURPOSE OF DISTRIBUTION

This document is electronically approved. Records regarding the signatures are stored in the Fuel BU Document Database. Any attempt to modify this file may subject employees to civil and criminal penalties. EDM Object Id: 09012167809aa5d0 Release date (YYYY/MM/DD) : 2016/10/04 22:04:50 [Western European Time]

Role	Name	Date (YYYY/MM/DD)	Organization
Writer	TUPPER Lawrence	2016/10/04 19:54:00	AREVA Inc.
Reviewer	ELLIOTT Kevin	2016/10/04 20:36:34	AREVA Inc.
Approver	MCQUADE Patrick	2016/10/04 22:04:43	AREVA Inc.

RELEASE DATA:

SAFETY RELATED DOCUMENT: Y

CHANGE CONTROL RECORDS:
This document, when revised, must be reviewed or approved by the following regions:

France:	N
USA:	Y
Germany:	N

Exportkennzeichnung AL: 0E001 ECCN: 0E001
Die mit "AL ungleich N" gekennzeichneten Güter unterliegen bei der Ausfuhr aus der EU bzw. innergemeinschaftlichen Verbringung der europäischen bzw. deutschen Ausfuhrgenehmigungspflicht. Die mit "ECCN ungleich N" gekennzeichneten Güter unterliegen der US-Reexportgenehmigungspflicht. Auch ohne Kennzeichen, bzw. bei Kennzeichen "AL: N" oder "ECCN: N", kann sich eine Genehmigungspflicht, unter anderem durch den Endverbleib und Verwendungszweck der Güter, ergeben.

Export classification AL: 0E001 ECCN: 0E001
Goods labeled with "AL not equal to N" are subject to European or German export authorization when being exported within or out of the EU. Goods labeled with "ECCN not equal to N" are subject to US reexport authorization. Even without a label, or with label "AL: N" or "ECCN: N", authorization may be required due to the final whereabouts and purpose for which the goods are to be used.

[redacted]

REVISONS

REVISION	DATE	EXPLANATORY NOTES
1.0	24 February 2014	Report NSA DAC AREVA 14 01 "Structural Analyses of the AREVA Atrium 11 LTA Fuel Assembly in the RAJ II Container during Normal and Accident Transport Conditions". This report was created by Nuclear Safety Associates under Purchase Authorization 83 9215737 000 of 26 November 2013.
2.0	See 1st page release date	Report NSA DAC AREVA 14 01 Rev 1 "Structural Analyses of the AREVA Atrium 11 LTA Fuel Assembly in the RAJ II Container during Normal and Accident Transport Conditions". This report was created by Nuclear Safety Associates under Purchase Authorization 83 9241222 000 of 2 June 2015. Changes to the report were: • Add report number to main report • Modify pages 2 4, 46 55 to reflect the addition of Appendix C and match the post processing methodology for calculating the pitch change as reported in Appendix C. • Add Appendix C. Update references.

ATKINS

Nuclear Safety Associates
Design Analyses and Calculation

Design Analysis and Calculation (DAC) No.: ATKINS-NS-DAC-AREVA-14-01 (NSA-DAC-AREVA-14-01 Rev 1)	Rev. No.: 1	Page No.: 1	Total Pages: 55
Structural Analyses of the AREVA Atrium-11 LTA Fuel Assembly in the RAJ-II Container during Normal and Accident Transport Conditions			

Scoping	☐	Preliminary	☐	Final	☒	Unverified Assumptions?	Yes	☐	No	☒

Objective:
This DAC documents the structural analyses of the AREVA Atrium-11 LTA fuel assembly in the RAJ-II Container during Normal Condition of Transport (NCT) as per 10 CFR71.71 and Hypothetical Accident Transport Condition (HAC) of transport as per 10 CFR71.73.

HAC Analyses for the accident conditions are simulated by the LSDYNA finite element dynamic simulation program with the accident time history (ATH) input derived from the actual drop test of RAJ-II container (BSG-T98-005, Jan 1998) performed by Japan Nuclear Fuel Co., Ltd in the Licensing Application to Japan Science and Technology Agency. The peak values of ATH are scaled up from the actual drop test results to assure that a minimum factor of safety of 1.4 is maintained.

The accident conditions are conservatively simulated using material properties corresponding to temperatures of -40°F and 150°F.

Results:
The structural analyses performed confirmed that the AREVA Atrium-11 LTA fuel bundle meets all the structural requirements of the 10 CFR 71.71 and 10 CFR 71.73 without gross deformation that can result in a criticality event.

Preparer (Print): Tony Chung	Preparer (Sign): Tony Chung	Date: 9/14/2016
Reviewer(Print): Robert Stephenson	Reviewer (Sign): Robt W Steph	Date: 9/14/2016
Reviewer (Print):A. Bruce DeWald	Reviewer (Sign):	Date: 9/15/2016
Project Lead Engineer/Manager (Print): David McDaniel	Project Lead Engineer/Manager (Sign): David McDaniel	Date:
Professional Engineer (Print): Robert Stephenson/Tony Chung	Professional Engineer (Sign): Robt W Steph Tony Chung	Date: 9/14/2016
PE Seal/Stamp	ATKINS This calculation is prepared by Atkins NS. for AREVA under the AREAVA PO 1015036950.	

[redacted]

Form NSA-EN-13-03 R0

[redacted]
Revision History Log

Rev.	Date	Revision Description/Reason
0	2/21/2014	Initial Issue
1	9/12/2016	Add report number to main report, Appendices A and B. Modify pages 2-4, 46-55 to reflect the addition of Appendix C and match the post processing methodology for calculating the pitch change as reported in Appendix C. Add Appendix C. Update references.

Form NSA-EN-13-03 R1

[redacted]

Table of Contents

APPENDICES

Form NSA-EN-13-03 R1

[redacted]

1.0 INTRODUCTION

1.1 Background/Purpose

This report summarizes the results of structural analyses of the AREVA Atrium-11 LTA fuel assembly in the RAJ-II Container during Normal Condition of Transport (NCT) of 10 CFR71.71 [Ref. 1] and Hypothetical Accident Transport Condition (HAC) of 10 CFR71.73 [Ref. 2].

HAC Analyses for the accident conditions are simulated by the LSDYNA finite element dynamic simulation program with the accident time history (ATH) input derived from the actual drop test of RAJ-II container (BSG-T98-005, Jan 1998) performed by Japan Nuclear Fuel Co., Ltd in the Licensing Application to Japan Science and Technology Agency. The peak values of ATH are scaled up from the actual drop test results to assure that a minimum factor of safety of 1.4 is maintained.

The accident conditions are conservatively simulated using material properties corresponding to temperatures of -40°F and 150°F.

A comparison of the analysis results with the actual drop tests performed for RAJ-II SAR Rev. 7 [Ref. 18] is presented in Section 7.8

An evaluation of Normal Conditions of Transport is provided in Appendix A. An evaluation of a container with less than full weight ballast is provided in Appendix B. A refined evaluation of pitch change is presented in Appendix C.

1.2 Limits of Applicability

The accident drop simulation is applicable only to the extent that the un-channeled Atrium-11 LTA fuel assembly is packaged in the standard TN-B1/RAJ-II container. Analysis is done with the total payload weight of two Atrium-11 LTA fuel assemblies to allow comparison to drop test data done with two fuel bundles. The weight of the Atrium-11 LTA fuel bundle is essentially identical to the weight of Atrium-10. For a single Atium-11 fuel bundle packaged in the TN-B1/RAJ-II container, the other cavity in the inner container of TN-B1/RAJ-II should be occupied by a ballast within the bounds of this analyses and appendix B. The packing material facing the Lower Tie Plate and the Top handle of the Atrium-11 fuel bundle is made of Balsa wood with a minimum thickness of 5.8-inches and its grain direction must be parallel to the longitudinal axis of the fuel bundle as shown in the applicable TN-B1/RAJ-II licensing drawings. The inner container of the TN-B1/RAJ-II will hold the Atrium-11 LTA fuel bundle. The sides of the fuel bundle will be surrounded with packing material made of Ethafoam.

Actual ATRIUM 11 LTA fuel shipments are anticipated to be done in the TN-B1/RAJ-II shipping container with a single element in each shipping container and a ballast (fuel channel, cage assembly with tie plates) having the equivalent peripheral envelope with no fissionable material in the other side of the container. The ballast may not have the weight of the ATRIUM 11 element. Appendix B of this DAC evaluates the reduction in weight of ballast compared to a full weight element or ballast.

All other analyses results for HAC and NCT are independent of the number of fuel assemblies in the container.

[redacted]

2.0 Conclusions

The loading of normal conditions of transport are bounded by the accident conditions therefore the results of normal condition of transport are qualified by analogy.

The accident conditions during the normal transport are analyzed either by meeting the stress or deformation limit to the extent that was below the design requirement for the reactor in-core performance limit.

The drop scenarios are qualified first by similarity comparison between the dynamic parameter of Atrium-11 LTA fuel bundle with that of the Atrium-10 fuel bundle that was drop tested by AREVA while packaged in the identical outer container of RAJ-II.

As part of the qualification of Atrium-11 LTA fuel bundle, the accident drops are simulated using the LSDYNA dynamic simulation finite element program using conservative material properties at temperatures (-40 deg F and 150 deg F) that are more restrictive than that required by 10 CFR71.73. The acceleration time history (ATH) for the simulation are taken from the instrumented results recorded in the actual drop tests performed by Japan Nuclear Fuel Co., Ltd in the Licensing Application of RAJ-11 shipping fuel bundle and shipping container package to Japan Science and Technology Agency. The peak values of ATH are amplified with a scale factor to achieve a minimum factor of safety on structural stability greater than 1.4.

The structural analyses performed confirmed that the AREVA Atrium-11 LTA fuel bundle meets all the structural requirement of the 10 CFR 71.71 and 10 CFR 71.73.

[redacted]

3.0 ANALYSIS METHODOLOGY

The Atrium-11 LTA fuel bundle (Ref. 3) is illustrated in Figure 3-1 through 3-2 below. The dimensions are in millimeter. The accident drop evaluation is performed using the finite element analysis program LSDYNA. The finite element models of the Atrium-11 LTA fuel bundle and the surrounding packing material from the RAJ-II container are discussed in detail in Section 7.1.

The dynamic boundary conditions are the impact velocity due to a drop from a height of 30-ft and the acceleration time history experienced by the fuel bundle at the inner compartment of the RAJ-II container. The acceleration time histories are taken from the accelerometer installed in the actual drop test preformed in Ref. 4. The dynamic simulations are performed conservatively with peak accelerations with a minimum factor of 1.4 based on the measured value from drop test results.

Drop tests required by 10 CFR71.73 are performed for temperatures at -20°F (Cold Condition) and 100°F (hot condition). The material properties used in the drop simulation are conservatively taken from cold temperature of -40°F and hot temperature of 150°F.

[redacted]

[redacted]

Figure 3-2 Section View of Atrium-11 Fuel Bundle

4.0 COMPUTER CODES USED IN THE ANALYSIS

The LSDYNA finite element analysis program is used for drop analysis of Atrium-11 LTA fuel bundle (Ref. 5). LSDYNA is a dynamic simulation finite element analysis program with non-linear material and geometry capability. The LSDYNA program is verified in Ref. 6 following NSA's QA program.

[redacted]

5.0 ASSUMPTIONS

5.1 Assumptions

The following assumptions are made in the present analysis.

- The Atrium-11 LTA fuel bundle is packaged inside the inner container of the TN-B1/RAJ-II shipping container. The total weight of the Atrium-11 LTA fuel bundle is essentially equal to that of Atrium-10. The other cavity of the TN-B1/RAJ-II inner container is occupied with a dummy weight that has the same weight as Atrium-11 LTA fuel bundle.
- Actual ATRIUM 11 LTA fuel shipments may be done in the TN-B1/RAJ-II shipping container with a single element in each shipping container and a ballast (fuel channel, cage assembly with tie plates) having the equivalent peripheral envelope with no fissionable material in the other side of the container. The ballast will may have the weight of the ATRIUM element. Appendix B evaluates the reduction in weight of ballast compared to a full weight element or ballast and its acceptability.
- The fuel pellets are not modeled in the present analysis. However, the weights of the fuel pellets are added to the cladding tubes.
- In the dynamic simulation, the side surfaces of the inside container is assumed to be elastic. This is conservative given the side surfaces of the inner container are made of Ethafoam material and a steel sheet liner.
- In the present analysis, individual fuel bundle without the container is directly dropped at a velocity equals to 527.5 in/sec (corresponds to a height of 30 ft). It results in conservative estimate of the damage of the fuel bundle as all the energy is to be absorbed by the fuel bundle. In reality, the inner container absorbs considerable energy. Therefore, the predicted response of the fuel bundle is very conservative.
- On both ends of the fuel bundle, the cushioning material is made of balsa wood blocks. In this report, the stiffness of the balsa wood is assumed to be equal to the stiffness of wood at cold temperature with grain direction parallel to the fuel bundle longitudinal axis. This is conservative so the greatest impact force can exert on the fuel bundle during the drop accident.
- Except for the end drop case, the fuel bundle is dropped on the rigid surface. It results in conservative estimate of damage of the fuel bundle. In reality, the fuel bundle impacts against the walls of the inner container which is deformable.
- The maximum acceleration from the Atrium-10 fuel bundle tests are scaled by a factor 1.4 to ensure a factor of safety of 1.4.
- As per 10 CFR71.73 the drop tests are to be performed at a temperature of -20°F (Cold Condition) and 100°F (hot condition). In the present analysis, the material properties used are conservatively taken at cold temperature of -40°F and hot temperature of 150°F.

[redacted]

6.0 ACCEPTANCE CRITERIA

6.1 Plastic Stability

The acceptance criteria for the plastic stability of fuel bundle are

a. During normal and accident temperature and pressure conditions, the fuel bundle cladding remains stable without gross deformation or collapse.

The evaluation of plastic stability of Atrium-11 LTA fuel bundle is done using the plastic load analysis methodology as per ASME Code [Ref. 7]. The above criteria are quantified by applying a minimum scale factor of 1.4 to the acceleration time histories from the RAJ-II container drop test results [Ref. 4] so that the minimum factor of safety is 1.4. The acceptance criteria for fuel bundle stability evaluation is established based on the acceptance criteria of the Plastic Instability Load Analysis as discussed in ASME Code Subsection III, Appendix F. Section F-1341.4 [Ref. 7]. The ASME Code states that the load should not exceed 70% of the plastic instability load. The criterion for the minimum safety factor for the Atrium-11 fuel bundle stability evaluation is considered to be 1.4 (1/0.7).

[redacted]

7.0 ANALYSES DETAILS

7.1 Fuel Bundle Finite Element Model

The fuel bundle inside the TN-B1/RAJ-II shipping container is surrounded by a foam material padding inside the inner container of the package [Ref. 8]. The padding is conservatively not included in the model and analysis. However, the balsa wood shock absorber at the bottom of the fuel bundle is included for the end drop analyses as shown in Figure 7.1-2. As explained in Section 5.0, the container is not modeled in the present analysis. The fuel bundle alone is directly dropped and it results in conservative prediction of the response of the fuel bundle. The finite element model details of the Atrium-11 LTA fuel bundle are shown in Figures 7.1-1 through 7.1-5 below.

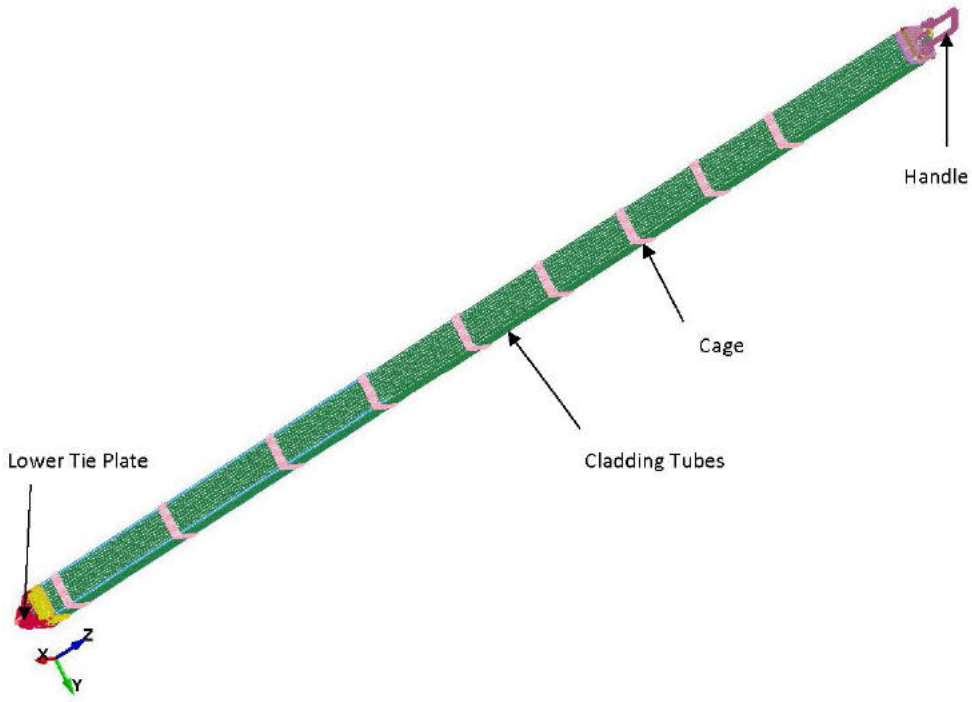

Figure 7.1-1 Finite Element Model of Atrium-11 LTA Fuel Bundle

Form NSA-EN-13-03 R1

[redacted]

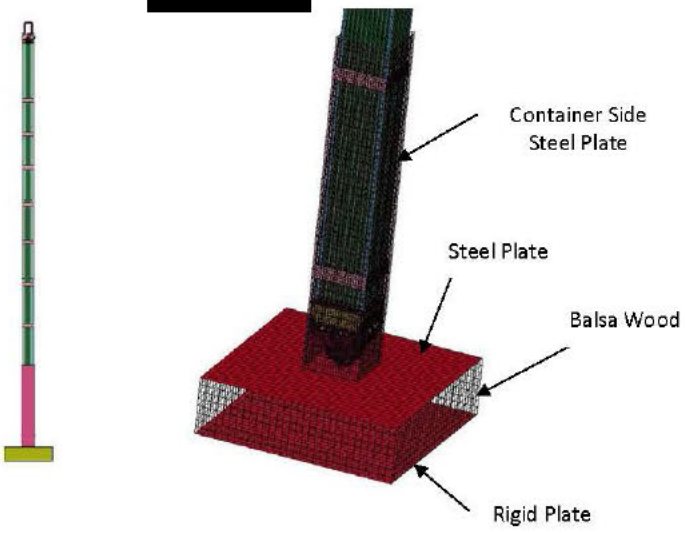

Figure 7.1-2 Finite Element Model of Atrium-11 LTA Fuel Bundle - End Drop

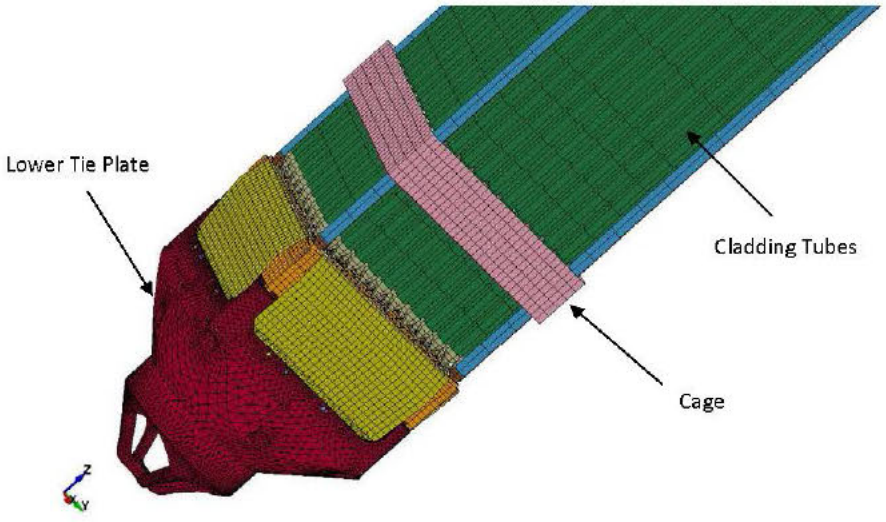

Figure 7.1-3 Finite Element Model - Atrium -11 LTA Fuel Bundle - Lower Region

Form NSA-EN-13-03 R1

[redacted]

Form NSA-EN-13-03 R1

[redacted]

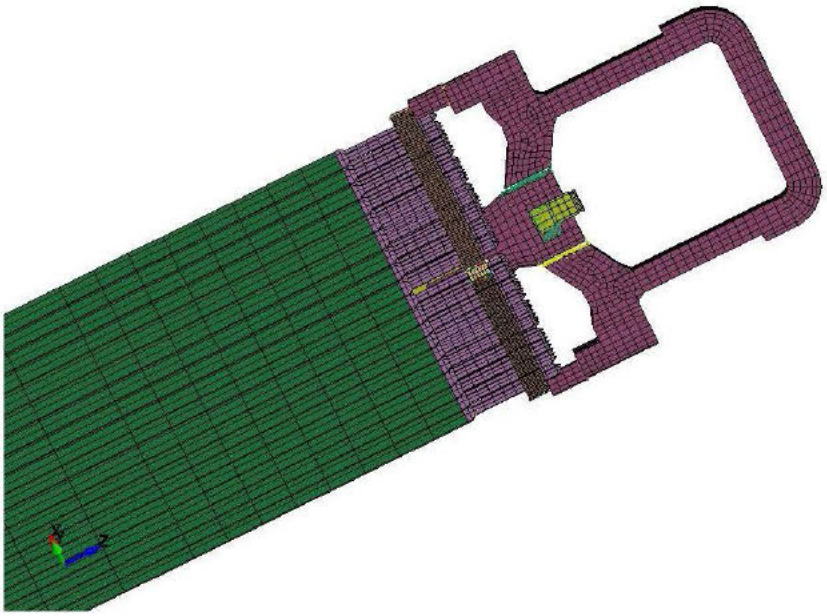

Figure 7.1-5 Finite Element Model - Atrium-11 LTA Fuel Bundle - Upper Bail Handle Region

Form NSA-EN-13-03 R1

7.2 Foam Padding Finite Element Model [redacted]

The Atrium-11 LTA fuel bundle is shipped in a TN-B1/RAJ-II package as shown in Figure 7.2-1 below. The cross section view of the RAJ-II package without the shock absorber (balsa wood) is shown in Figure 7.2-2 below.

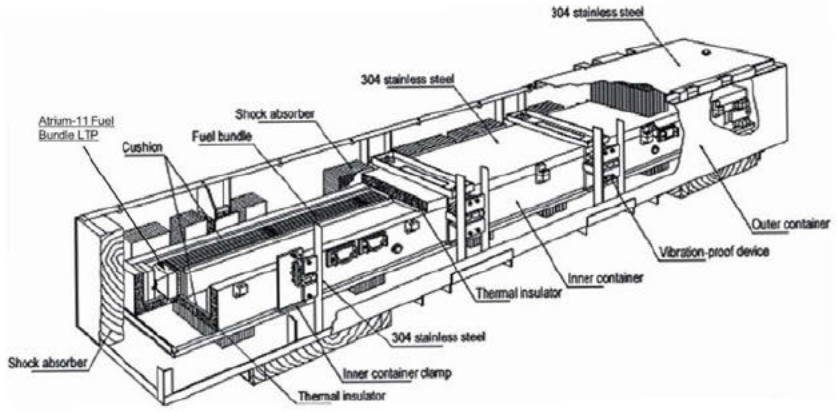

Figure 7.2-1 RAJ-II Shipping Package

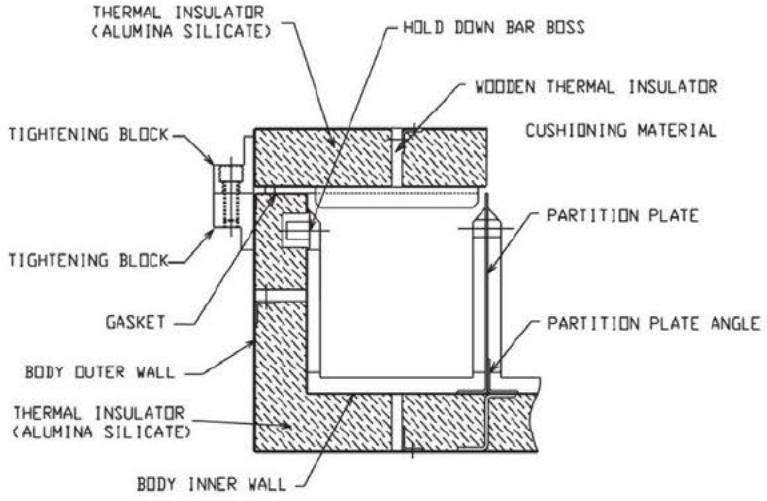

Figure 7.2-2 RAJ-II Cross Section View of RAJ-II inner Container

Surrounding the fuel bundle in the inside container of RAJ-II are the foam paddings that consist of cushions, thermal insulators and shock absorbers. The stainless steel sheets surrounding the thermal insulators are not modeled. The shock absorbers on both ends are made of balsa wood. The shock absorbers for the side drop protection are made of paper honeycomb. The cushions are made of polyethylene foam (Ethafoam).

The thermal insulator is made of filled aluminum silicate. The lateral foam paddings are conservatively not represented in the finite element model of side drops and CG-over-Corner Drop analyses. The longitudinal balsa wood block is included in the end drop analysis model. The physical placements of foams in the container are illustrated in Figure 7.2-3 and Figure 7.2-4.

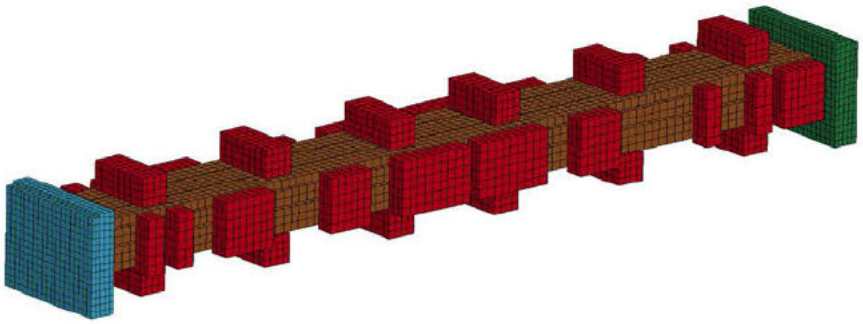

Figure 7.2-3 Shock Absorbers Surrounding the Fuel Bundle

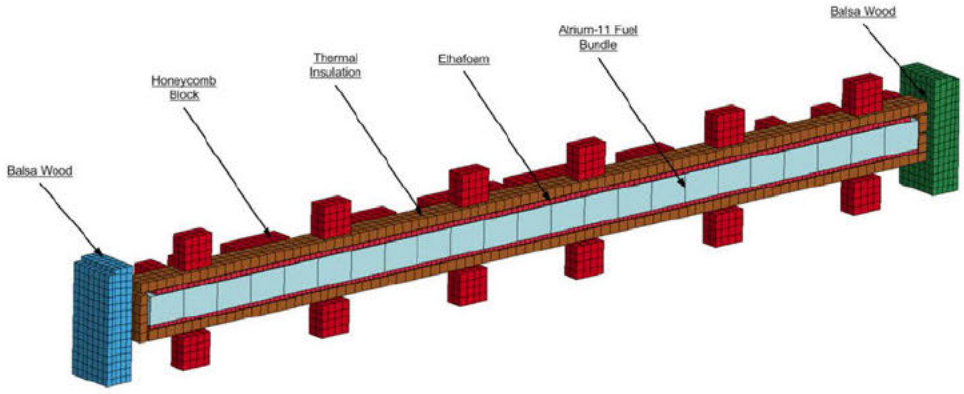

Figure 7.2-4 Cutaway View of the Foam Paddings Surrounding the Fuel Bundle

7.3 Material Properties

The materials used in the Atrium-11 LTA fuel bundle and the relevant cushioning material that are included in the finite element model are discussed below.

[redacted]

7.3.1 Zircaloy-2

Per Ref. 9, Section 1.1.2, the material used in the AREVA Atrium-11 LTA fuel bundle is ASTM grade R60802 (Zircaloy-2), the orientation dependency of the material used in the fuel tubes is not specified. The ultimate and yield stresses are listed in Ref. 9, Section 3.3.1 as follows.

Table 7.3.1-1 Mechanical Properties of Zircaloy-2 from Ref. 9

Property	Room Temperature	382°C (720°F)
Ultimate Tensile Stress, ksi	78	42
Yield Stress, ksi	55	30
Elongation, %	16	16

The LSDYNA input requires the strain-rate sensitive stress strain curve and the Poisson's ratio at the boundary temperature condition. At high strain rate, as in the case of dynamic impact condition, the yield stress increases which tend to strengthen the material. It is conservative in the impact analysis to ignore the strain-rate effects and use the static material properties.

ASME CODE STANDARDS

Ref. 10 provide the material model for different alloys to generate the stress strain curve at temperature of interest based on the modulus of elasticity, E_y, the engineering yield stress, σ_{ys}, and engineering ultimate tensile stress, σ_{uts}. For the present analysis, all of the above properties are evaluated at temperature of interest (-40°F and 150°F). The yield stress and ultimate tensile stress are derived by interpolation from Ref. 11 and listed in Table 7.3.1-2 below. The Poisson's ratio does change significantly with alloying; therefore the Poisson's ratio listed in Ref. 12 as 0.35 is applicable to Zirconium-2, which is used for BWR fuel cladding.

MODULUS OF ELASTICITY OF ZIRCONIUM-2

Ref. 12 listed the experiment work of measuring the elastic modulus in the longitudinal orientation and compared with the Canadian Standard CSA N285.6 for R60802 seamless tubes. The following equation is proposed.

$$E=98.37-0.06595 \times T-1.33 \times 10^{-5} \times T^2 - 5.902 \times 10^{-8} T^3$$

Where E is in GPa, T is in °C. Following the equation above, the modulus of Elasticity at -40°F (-40°C) is:

$$E = 100.99 \text{ GPa} = 14.65 \times 10^6 \text{ psi.}$$

The modulus of Elasticity at 150°F (65.5°C) is:

$$E = 93.97 \text{ GPa} = 13.63 \times 10^6 \text{ psi.}$$

[redacted]

Table 7.3.1-2 Mechanical Properties of Zircaloy-2 at temperature of interest

Property	-40°F	150°F
Modulus of Elasticity, ksi	14,650	13,630
Ultimate Tensile Stress, ksi	87.21	71.30
Yield Stress, ksi	61.4	50.35
Elongation, %	14.5	14

The stress strain curves based on Ref. 10 are plotted as follows.

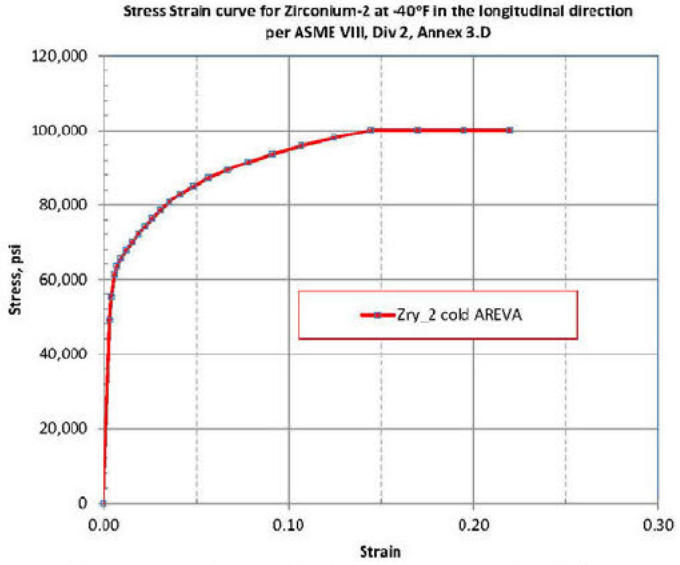

Figure 7.3.1-1 Stress Strain Curves for Zircaloy-2 at -40°F

Form NSA-EN-13-03 R1

[redacted]

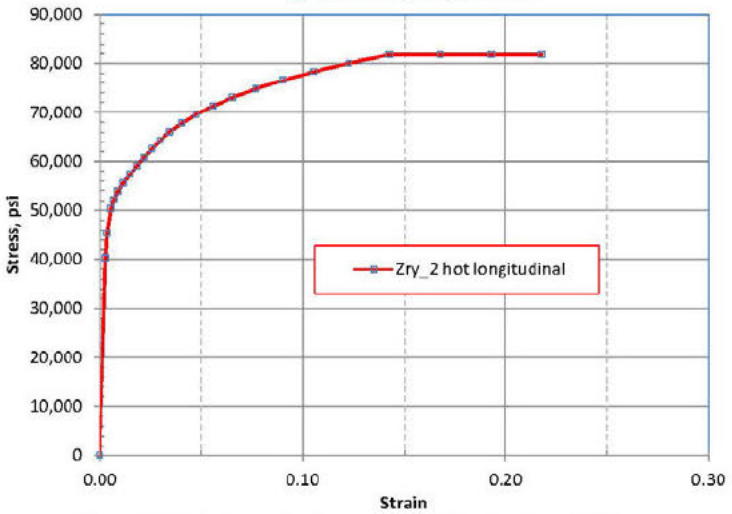

Figure 7.3.1-2 Stress Strain Curves for Zircaloy-2 at 150°F

7.3.2 SS304L

The material properties for 304L are presented in Table 7.3.2-1 below.

Table 7.3.2-1 Mechanical Properties of 304L at temperature of interest

Property	-40°F	150°F	Reference
Modulus of Elasticity, E , ksi	28,900	27,800	Ref. 13 , Table TM-1
Ultimate Tensile Stress, S_u, ksi	65	62.7	Ref. 13, Table U
Yield Stress, S_y, ksi	25	22.7	Ref. 13, Table Y-1
Elongation, %	46.5	48	Derived from S_u and E

The stress strain curves at temperature of interest based on the table above and the equations in Ref. 10 are plotted as follows.

[redacted]

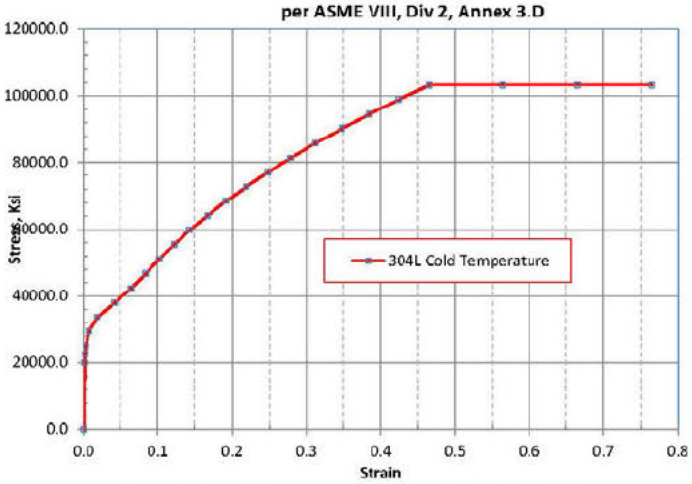

Figure 7.3.2-1 Stress Strain Curves for 304L at -40°F

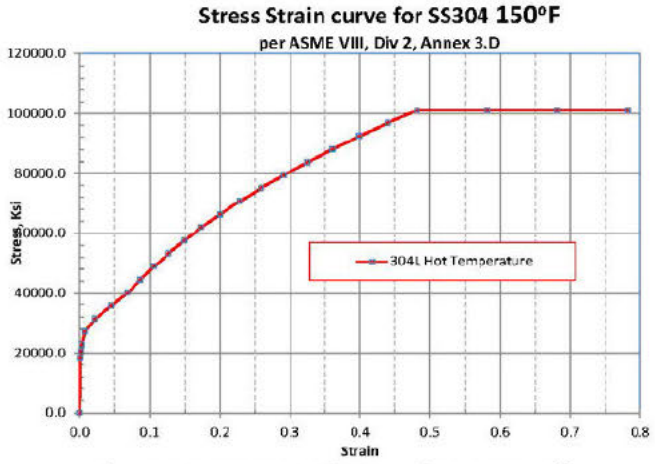

Figure 7.3.2-2 Stress Strain Curves for 304L at 150°F

Form NSA-EN-13-03 R1

[redacted]

At high strain rate, as in the case of dynamic impact condition, the yield stress increases which tend to strengthen the material. The Strain-rate Sensitivity of 304L, taken from Ref. 14 and 15, are listed in Table 7.3.2-1 below. The strain rate sensitivity data for 304L at temperature of -40°F is the same as that at temperature -20°F.

Table 7.3.2-1 The Strain-rate Sensitivity of 304L

Strain Rate	Temperature, °F				
	-20	70	150	300	600
5	1.333	1.235	1.211	1.166	1.043
10	1.361	1.278	1.254	1.210	1.094
22	1.428	1.381	1.358	1.316	1.217
25	1.445	1.407	1.384	1.342	1.247

7.3.3 Balsa Wood

Balsa wood is used for primary impact protection during the end drop.

The ambient and cold temperature properties are taken from the stronger parallel to grain direction [Ref. 16]. The ambient curve is benchmarked in Ref. 17 from the crush measured following the end drop. To ensure that the maximum acceleration is achieved, the cold properties are increased by approximately 30%. The Benchmarking of the balsa properties is discussed in Ref. 17 and below.

Benchmarking of the balsa properties was accomplished by comparing the measured crush to the LS-DYNA model. To make the comparison, a core sample measurement of the end drop CTU was made. The core sample showed that the balsa block crushed 2 inches, which agrees with the LS-DYNA results.

The Balsa woods are modeled using the LS-DYNA material *MAT_CRUSHABLE_FOAM. The stress strain properties used in this analysis are presented in Table 7.3.3-1 below. The stiffness of the wood is conservatively increased 10% in the analysis.

Table 7.3.3-1 Balsa Wood True Stress versus Strain Properties

Relative volume	Stress at 77°C	Stress at 21°C	Stress at -40°C
0.000	0	0	0
0.010	66	665	1500
0.025	90	1065	1900
0.050	98	1265	2000
0.075	100	1365	2010
0.100	102	1405	2020
0.200	110	1555	2060
0.300	118	1695	2160
0.400	126	1835	2260
0.500	134	1980	2360
0.600	153	2260	2710
0.700	360	4260	7218

7.4 Drop Configurations

[redacted]

The drop configurations are selected to comply with the requirements of 10 CFR 71.73(1) [Ref. 2]. The orientations with the most potential for damaging are selected. The drop orientations coincide with those orientations selected by actual drop test in the previous licensing application of RAJ-11 package to the Japanese regulator authority [Ref. 4]. From this referenced report, the measured acceleration time histories become the basis for this dynamic simulation.

The selected drop configurations are listed in Table 7.4-1 below.

Table 7.4-1 Drop Cases Configurations

Drop Case ID	Cask Orientation	Acceleration Time History And packaging material Temperature Condition	Atrium Fuel Bundle Material Property
1A	Side Drop	Side Drop, Cold	Cold
1B	Side Drop	Side Drop, Cold	Hot
2A	Bottom End Drop	End Drop, Cold	Cold
2B	Bottom End Drop	End Drop, Cold	Hot
3A	CG Over Corner Drop	Corner Drop, Cold	Cold
3B	CG Over Corner Drop	Corner Drop, Cold	Hot

The photos from Ref. 4 illustrating the 3 TN-B1/RAJ-II container drop orientations inside which the Atrium-11 LTA fuel bundle will be shipped are shown in Figures 7.4-1 through Figure 7.4-3 below.

ATKINS-NS-DAC-AREVA-14-01 (NSA-DAC-AREVA-14-01)
Rev. 1
Page 22 of 55

[redacted]

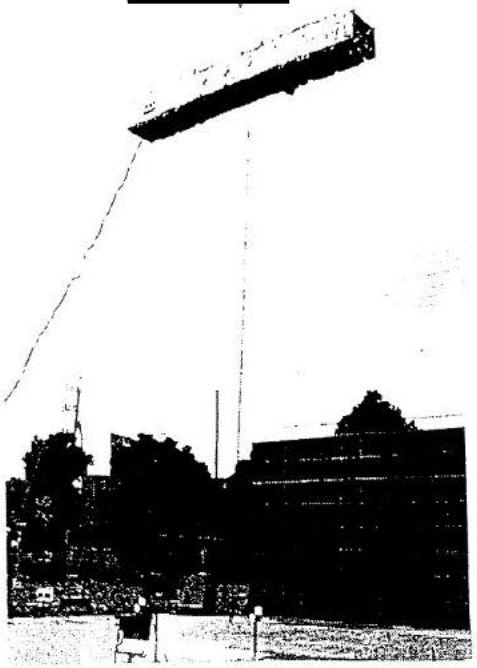

Photo (B)-A.19 Lid face horizontal drop (Before drop)

Figure 7.4-1 RAJ-II Container Position of Side Drop Configuration

Form NSA-EN-13-03 R1

[redacted]

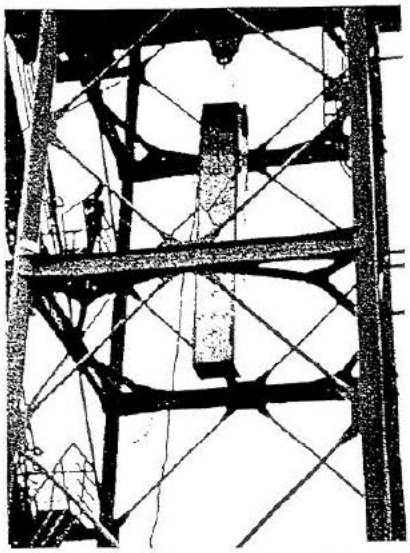

Photo (B)-A.13 Lower face vertical drop (Before drop)

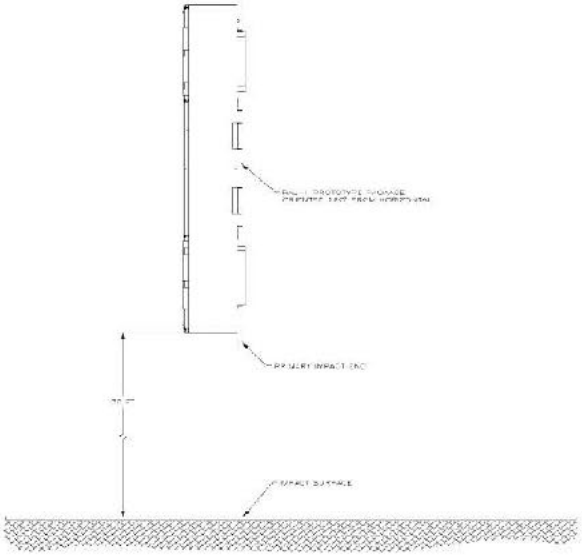

Figure 7.4-2 RAJ-II Container Position of Vertical End Drop

[redacted]

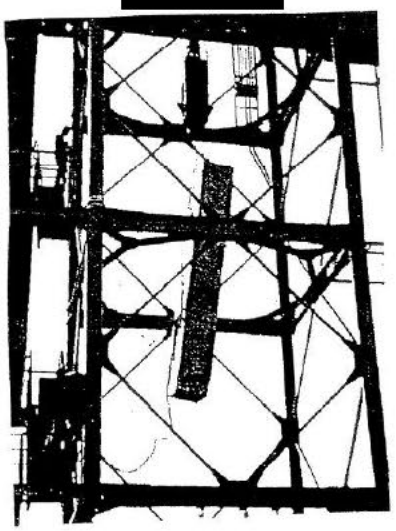

Photo (B)-A.8 Upper bottom face corner drop (Before drop)

Figure 7.4-3 RAJ-II Container Position of CG Over Corner Drop, the Longitudinal Axis is 6° off Vertical Plumb

Form NSA-EN-13-03 R1

[redacted]

7.5 Acceleration Time History

The drop test [Ref. 4] performed for the RAJ-II Certified Test Unit (CTU) [Ref. 18] listed the instrumented test results of the acceleration time histories during a 30-ft drop as follows.

Table 7.5-1 Acceleration Result from GNJ-J Certified Test Unit (CTU) during HAC Drop Test

Drop Orientation	Acceleration	Sensor Location	Reference
HAC free drop, vertical bottom end	303G	Inner container's outer shell	Ref. 4, page (B)A-122 Fig.(B)-A App. 6
HAC free drop, horizontal top drop on lid	146 G	Spacer of Center of fuel bundle	Ref. 4, page (B)A-124 Fig.(B)-A App. 8
HAC free drop, horizontal top drop on lid	194G	Inner container's outer shell	Ref. 4, page (B)A-125 Fig.(B)-A App. 9
HAC free drop, CG-over bottom end lower corner	203 G	Lower Tie Plate of Fuel Bundle	Ref. 4, page (B)A-120 Fig.(B)-A App. 4

The original instrument output and digitized acceleration time histories for the bounding side drop, end drop and corner drops are shown in Figure 7.5.1-1, Figure 7.5.2-1 and Figure 7.5.3-1 respectively. The predicted peak accelerations reported by RAJ-II SAR Rev.8 [Ref. 17] using LSDYNA program are listed below.

Table 7.5-2 Acceleration Time-Histories reported by LSDYNA analysis [Ref. 17] output

Drop Description and condition	Result	Reference, section and page number
Side Drop at -40°C (-40°F)	339.6 G	Ref.17, page 2-101
Bottom End Drop at -40°C (-40°F)	377.8 G	Ref. 17, page 2-102
CG Over Corner Drop at -40°C (-40°F)	227.7 G	Ref.17, page 2-102

For the current hypothetical drop simulation, the peak accelerations are conservatively scaled up to bound both the actual drop test and dynamic simulation results. Since the analysis is performed using the plastic load analysis methodology, plastic stability of the Atrium-11 LTA fuel bundle and the lower tip plate is required by ASME Code [Ref. 7]. The above criteria are implemented by applying a minimum scale factor of 1.4 to the acceleration time histories from the RAJ-II container drop test result [Ref. 4] presented in Table 7.5-1 above so the minimum factor of safety is 1.4. The acceptance criteria for fuel bundle stability evaluation is established based on the acceptance criteria of the Plastic Instability Load Analysis as discussed in ASME Code Subsection III, Appendix F. Section F-1341.4 [Ref. 19]. The ASME Code states that the load should not exceed 70% of the plastic instability load. The criterion for the minimum safety factor for the Atrium-11 LTA fuel bundle stability evaluation is considered to be 1.4 (1/0.7). The analyzed peak accelerations for the drop cases are listed in Table 7.5-3 below. The plots illustrating the measured acceleration time histories (ATH) and the magnified ATH used in the current analyses are shown in Sections 7.5.1 through 7.5.3 below.

The ATH corresponds to an initial velocity of 527.45 in/sec as shown in Section 7.6. By applying the ATH to an object falling at an initial velocity of 527 in/sec, the terminal velocity should be zero at the end of impact. Scaling up the actual ATH at its peak value generates a permanent upward residual velocity that does not agree with the actual drop event. Therefore the digital ATH curve is trimmed after the peak value to reach a zero terminal velocity after the impact event. The corrected ATHs for each drop simulation are presented in each of the subsections.

[redacted]

Table 7.5-3 Acceleration Time-Histories input and Factors of Safety

Drop Orientation	Peak Acceleration For LSDYNA input	Figure	Peak Acceleration from Drop Test results	Factor Of Safety
Side Drop	350 G	7.5.1-2	194 G	1.8
Bottom End Drop	424 G	7.5.2-2	303 G	1.4
CG Over Corner Drop	284 G	7.5.3-2	203 G	1.4

[redacted]

7.5.1 Side Drop

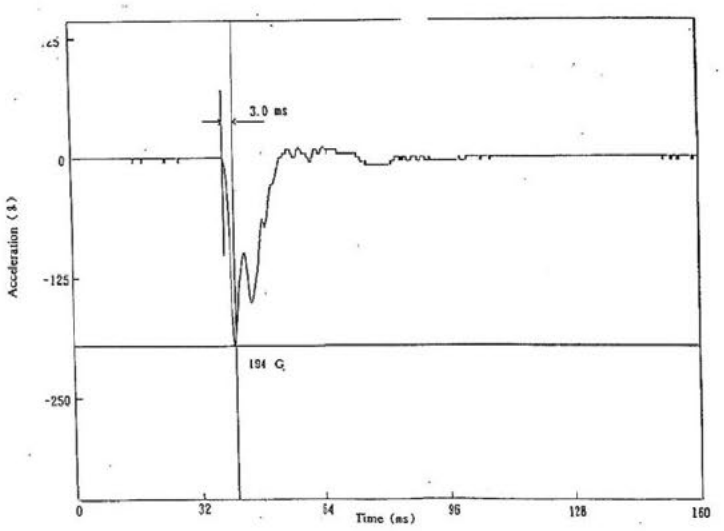

Figure 7.5.1-1 Acceleration wave-form in 9m Side Drop, filtered at 500 Hz [Ref. 4, page (B)A-125]

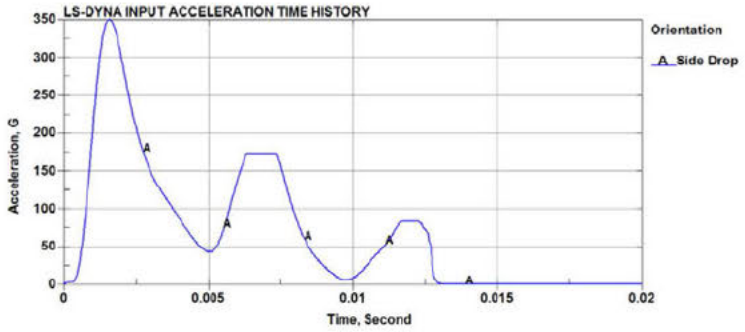

Figure 7.5.1-2 Acceleration Time History Input for Side Drop

Form NSA-EN-13-03 R1

[redacted]

7.5.2 End Drop

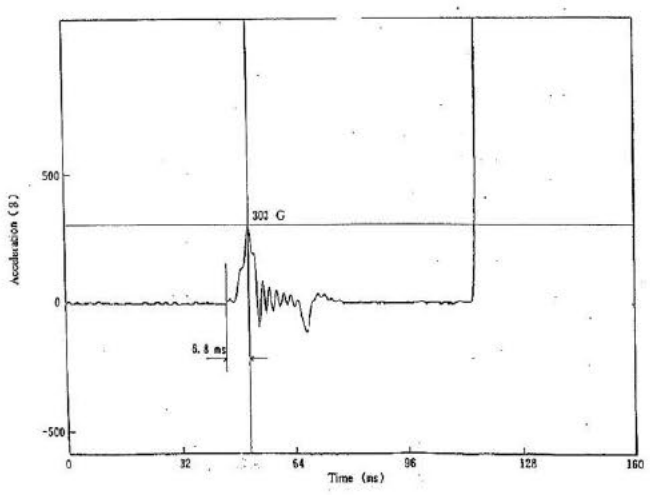

Figure 7.5.2-1 Acceleration wave-form in 9m Vertical drop, filtered at 500 Hz [Ref. 4, page (B)A-122]

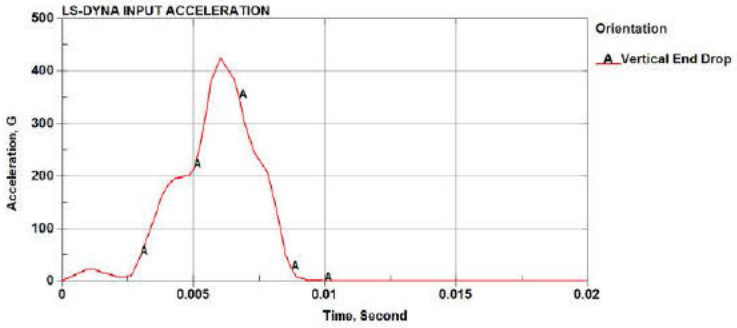

Figure 7.5.2-2 Acceleration Time History Input for Vertical Drop

Form NSA-EN-13-03 R1

[redacted]

7.5.3 CG Over Corner Drop

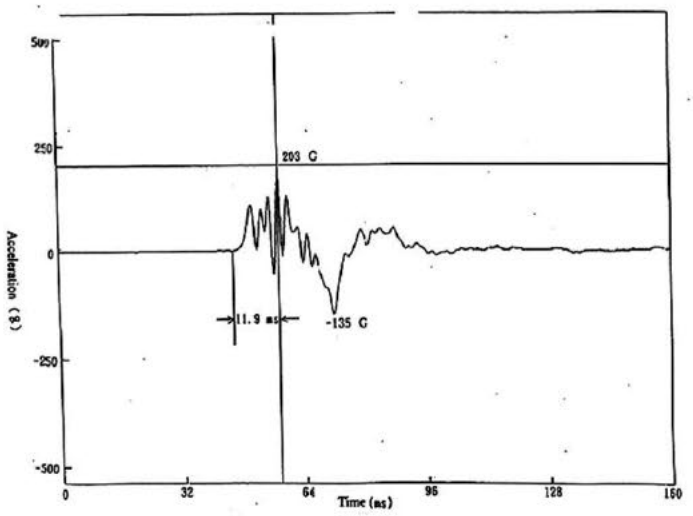

Figure 7.5.3-1 Acceleration wave-form in 9m Corner Over Corner drop, filtered at 500 Hz [Ref. 4, page (B) A-120]

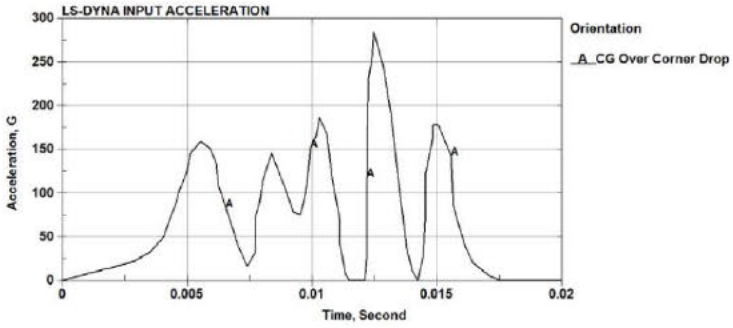

Figure 7.5.3-2 Acceleration Time History Input for CG Over Corner Drop

7.6 [redacted] Initial Velocity and Gravity Load

The initial velocity is determined by the drop height of 30-ft so that the kinetic energy equals the potential energy.

$$V=\sqrt{2 \times g \times h} = \sqrt{2 \times 386.4 \times 360} = 527.45 \text{ in/sec.}$$

Where

g=gravitational constant = 386.4 in/sec^2
h= drop height = 30 ft = 360 in.

At the initiation of impact, the gravity and the initial velocity is applied to all parts of the fuel bundle finite element model. The acceleration time history is applied to the part representing the inner container of the TN-B1/RAJ-II package.

The gravity load acting on the fuel bundle is considered in the present analysis and is applied as a body load.

The weight of the Atrium-11 LTA fuel bundle used in the present analysis is equal to 584 lbs.

[redacted]

7.7 Finite Element Analyses Results

As shown in Table 7.4-1, the drop conditions are analyzed for both cold (-40 deg F) and hot (150 deg F) conditions.

The results for each drop orientation and temperature conditions are discussed below.

NOTE: Except for end drop cases, the surface against which the fuel bundle impacts is assumed to be rigid. In reality, the impact surface is soft (i.e., the inner surface of the inner container). The predicted deformation/damage is very conservative.

7.7.1 Side Drop

7.7.1.1 Cold Condition - Case 1A

The model set up for the side drop cold condition is shown in Figure 7.7.1.1-1. The surface on which the fuel bundle is dropped is assumed to be rigid. Use of rigid surface results in conservative deformation/ damage to the fuel bundle and the predicted response is very conservative.

Figure 7.7.1.1-1: Model Set-UP - Side Drop - Cold Condition

The deformed shape of the fuel bundle under side drop cold condition is shown in Figure 7.7.1.1-2. As can be seen, the lower end of the fuel bundle suffers some damage but the cladding tubes maintain their integrity. The cladding tubes bend and some of them slip out of the lower tie plate support at the bottom. The top cage at the top, supporting the cladding tubes also slides away but still keeps the tubes in place. The fuel is contained inside and is not exposed.

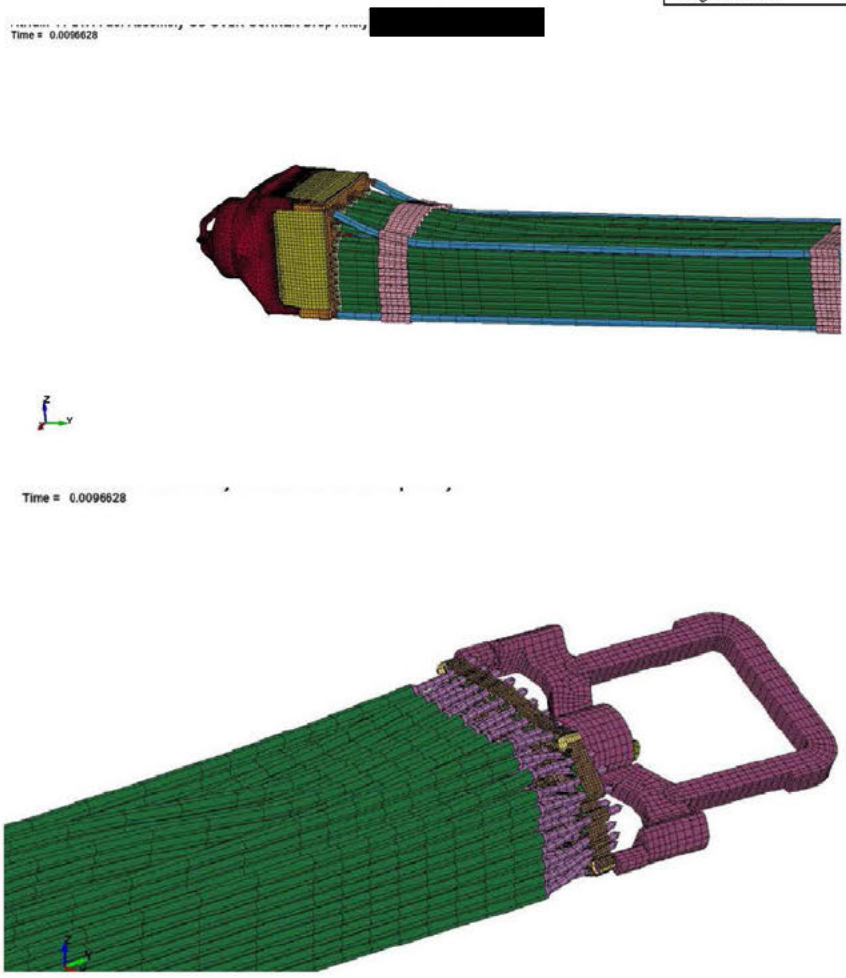

Figure 7.7.1.1-2: Deformed Shape - Side Drop - Cold Condition

7.7.1.2 Hot Condition - Case 1B

The model set up for the side drop hot condition is shown in Figure 7.7.1.2-1. The surface on which the fuel bundle is dropped is assumed to be rigid. Use of rigid surface results in conservative deformation/ damage to the fuel bundle and the predicted response is very conservative.

[redacted]

Figure 7.7.1.2-1: Model Set-UP - Side Drop - Hot Condition

The deformed shape of the fuel bundle under side drop hot condition is shown in Figure 7.7.1.2-2. As can be seen, the lower end of the fuel bundle suffers some damage but the cladding tubes maintain their integrity. The cladding tubes bend and some of them slip out of the lower tie plate support at the bottom. The top cage at the top, supporting the cladding tubes also slides away but still keeps the tubes in place. The fuel is contained inside and is not exposed.

[redacted]

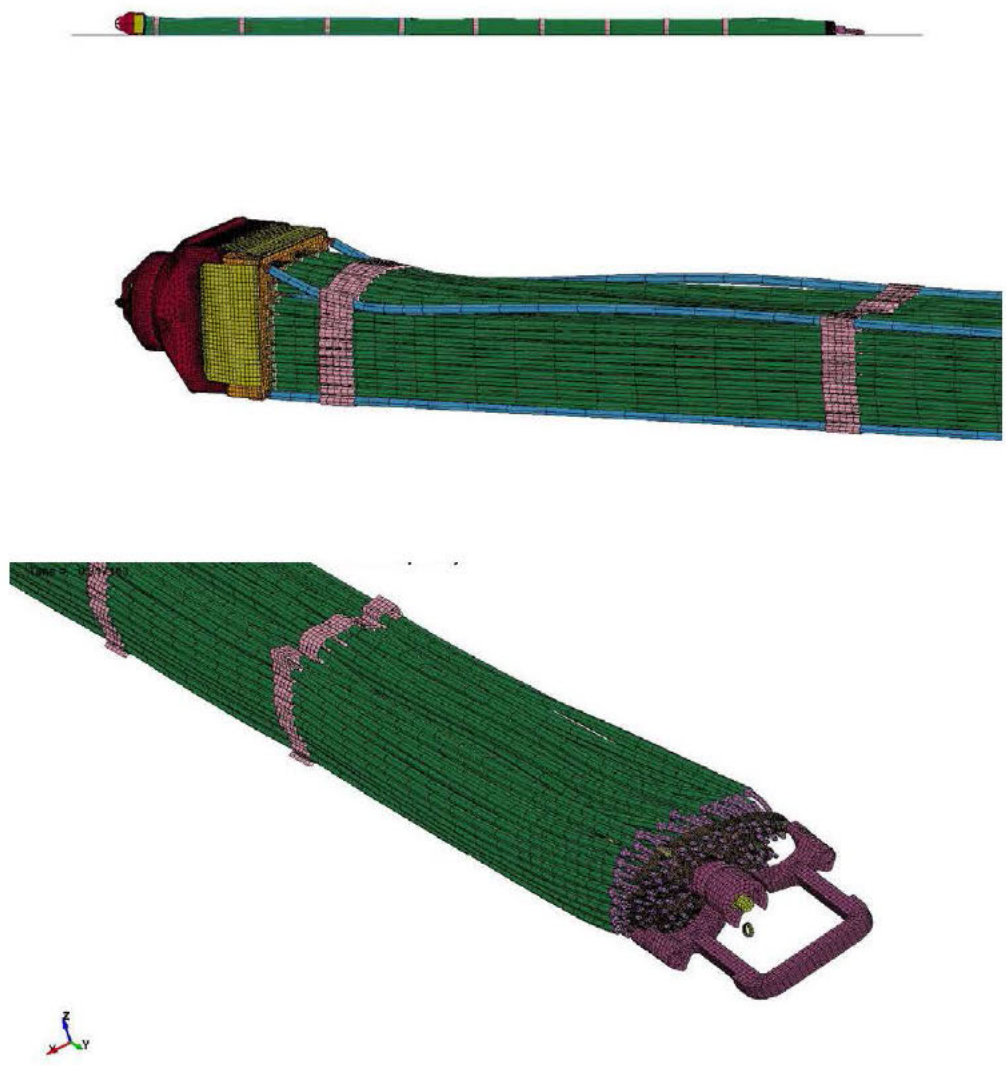

Figure 7.7.1.2-2: Deformed Shape - Side Drop - Hot Condition

Form NSA-EN-13-03 R1

[redacted]

7.7.2 Bottom End Drop

7.7.2.1 Cold Condition - Case 2A

The model set up for the bottom end drop cold condition is shown in Figure 7.7.2.1-1. In this case, the container end walls are modeled as a sandwich structure with two layers of metal plates to represent the inner container inside and outside plates and the Balsa wood material sandwiched between the plates. The inner plate is modeled using SS304L, whereas, the outer plate is modeled as rigid body. Also the lower portion of the fuel bundle is covered by a thin sheet of SS304L sheet representing the portion of the walls of the inner container.

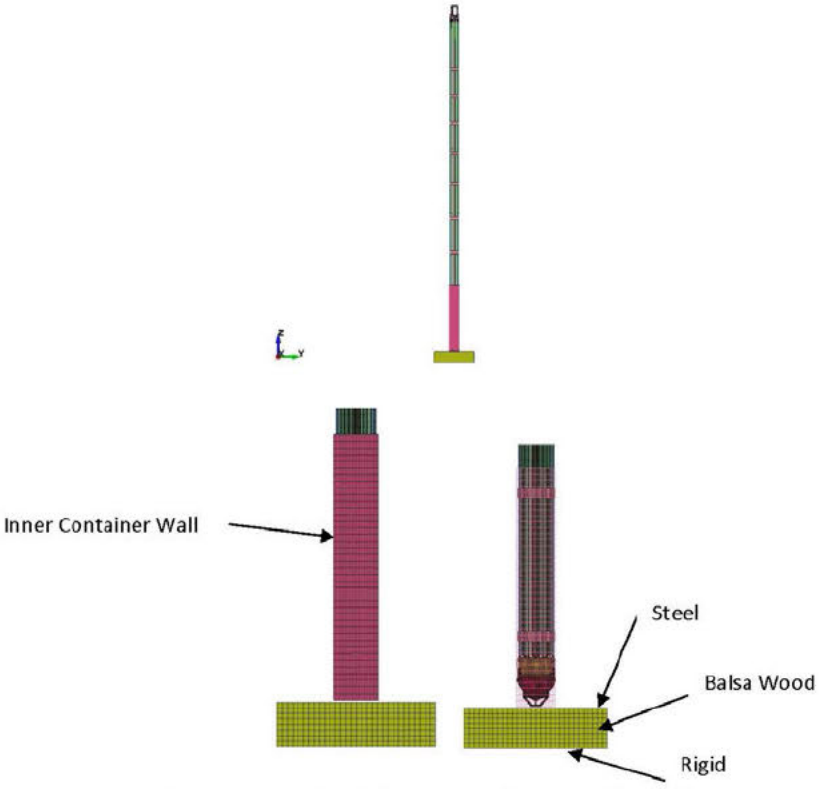

Figure 7.7.2.1-1: Model Set-Up - End Drop - Cold Condition

The deformed shape of the fuel bundle is shown in Figure 7.7.2.1-2. As can be seen the lower part suffers damage and the deformed shape of the fuel bundle is shown in Figure 7.7.2.1-2. The cladding tubes bend especially near the lower end, however, the cladding tubes maintain their integrity and the fuel inside the cladding tubes are contained.

[redacted]

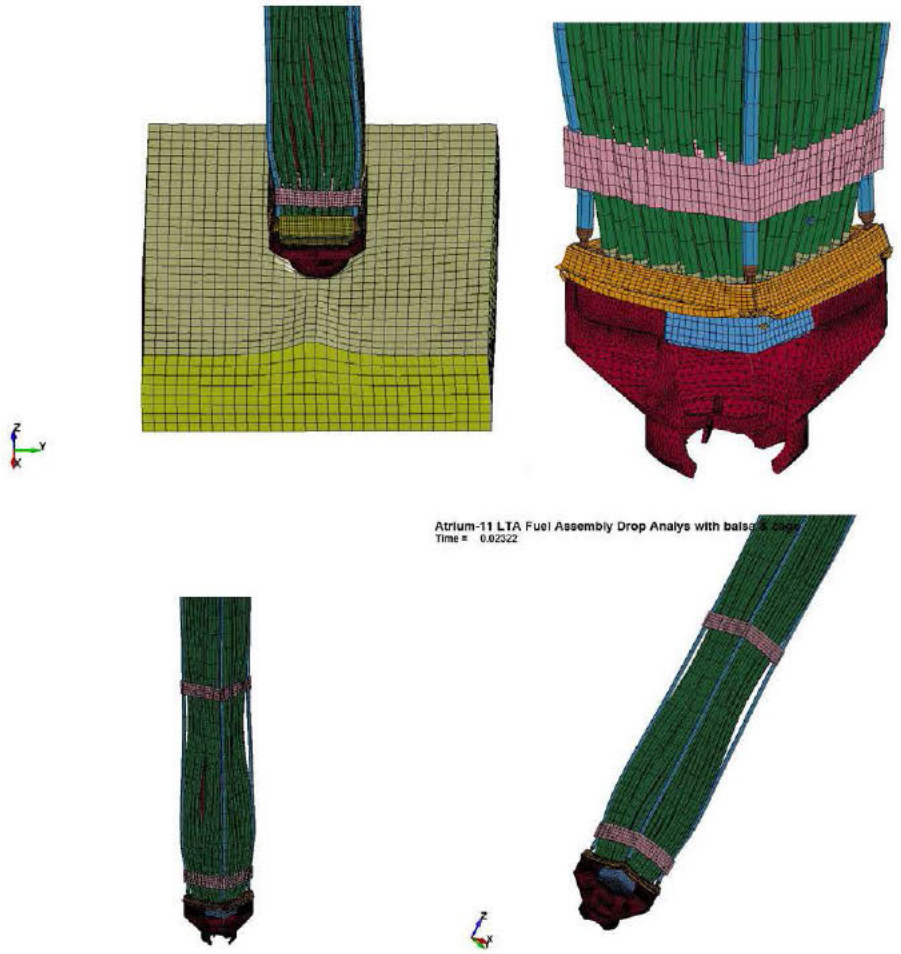

Figure 7.7.2.1-2: Deformed Shape - End Drop - Cold Condition

7.7.2.2 Hot Condition - Case 2B

The model set up for the bottom end drop hot condition is shown in Figure 7.7.2.2-1. As in the cold case, the container end walls are modeled as a sandwich structure with two layers of metal plates to represent the inner container inside and outside plates and the Balsa wood material sandwiched between the plates. The inner plate is modeled using SS304L, whereas, the outer plate is modeled as rigid body. Also the lower portion of the fuel bundle is covered by a thin sheet of SS304L sheet representing the portion of the walls of the inner container.

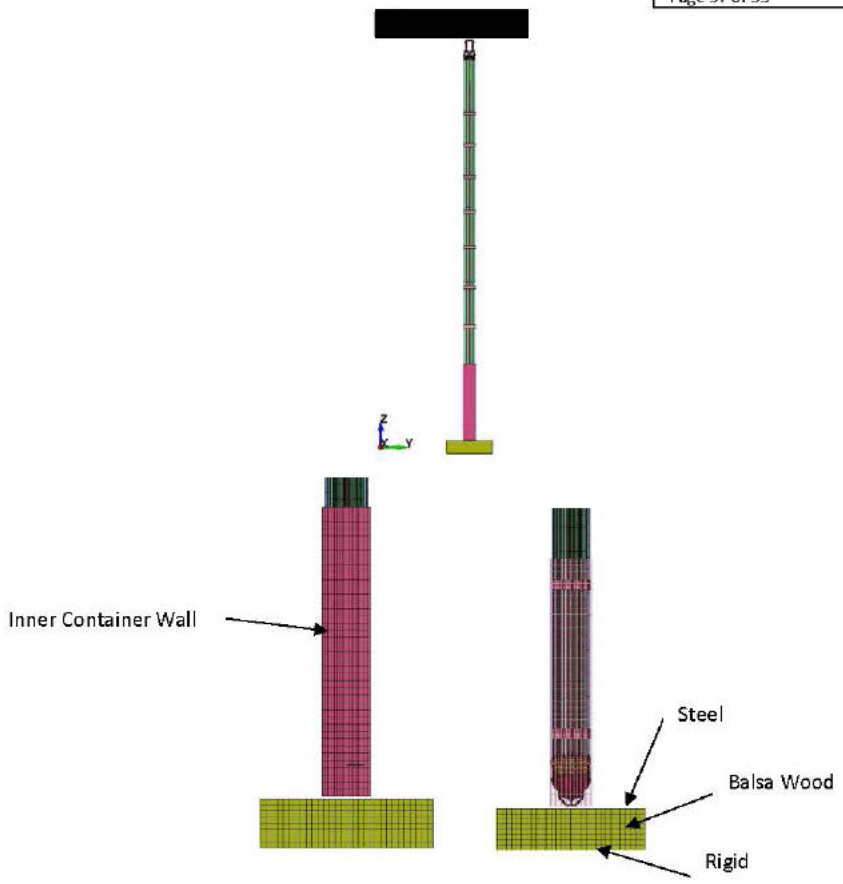

Figure 7.7.2.2-1: Model Set-Up - End Drop - Hot Condition

The deformed shape of the fuel bundle is shown in Figure 7.7.2.2-2. As can be seen the lower part suffers damage and the deformed shape of the fuel bundle is shown in Figure 7.7.2.2-2. The cladding tubes bend especially near the lower end, however, the cladding tubes maintain their integrity and the fuel inside the cladding tubes are contained.

[redacted]

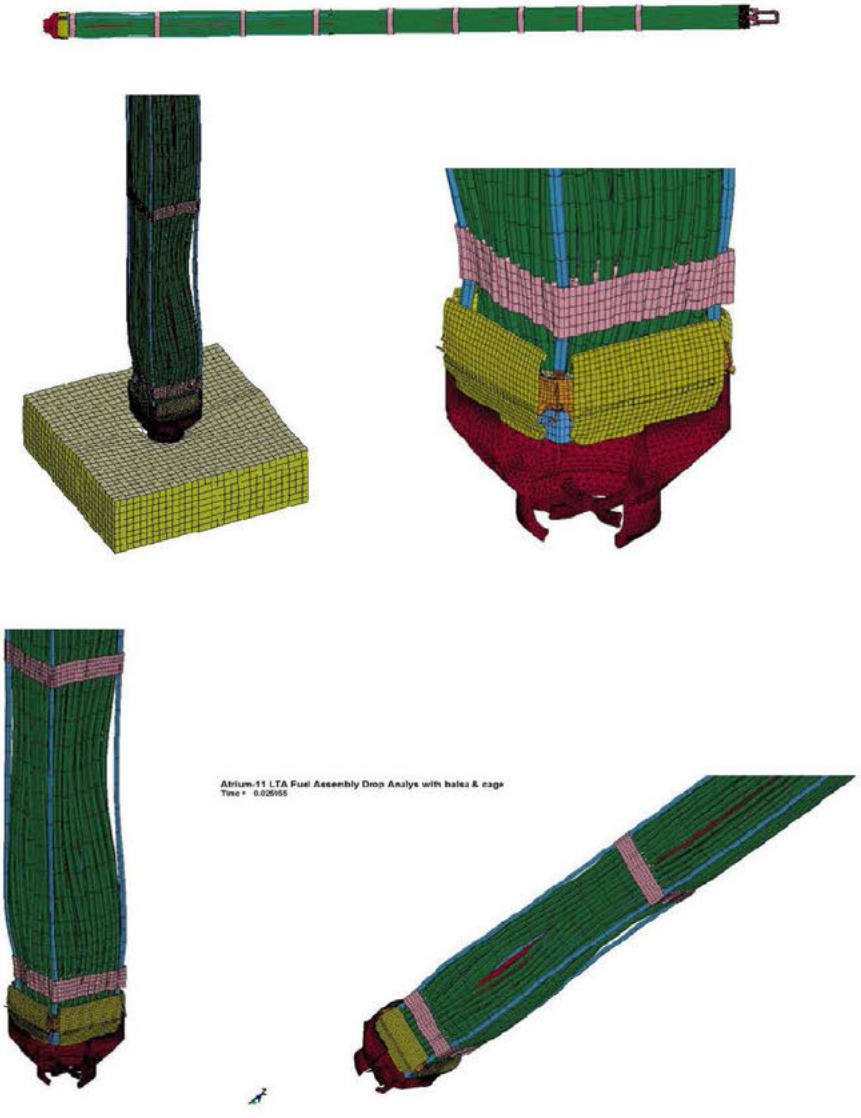

Figure 7.7.2.2-2: Deformed Shape - End Drop - Hot Condition

Form NSA-EN-13-03 R1

[redacted]

7.7.3 CG Over Corner Drop

7.7.3.1 Cold Condition - Case 3A

The model set up for the CG over corner drop cold condition is shown in Figure 7.7.3.1-1. The fuel bundle is inclined about 6 deg with vertical. The surface on which the fuel bundle is dropped is assumed to be rigid. Use of rigid surface results in conservative deformation/ damage to the fuel bundle and the predicted response is very conservative. Also the lower portion of the fuel bundle is covered by a thin sheet of SS304L sheet representing a portion of the walls of the inner container.

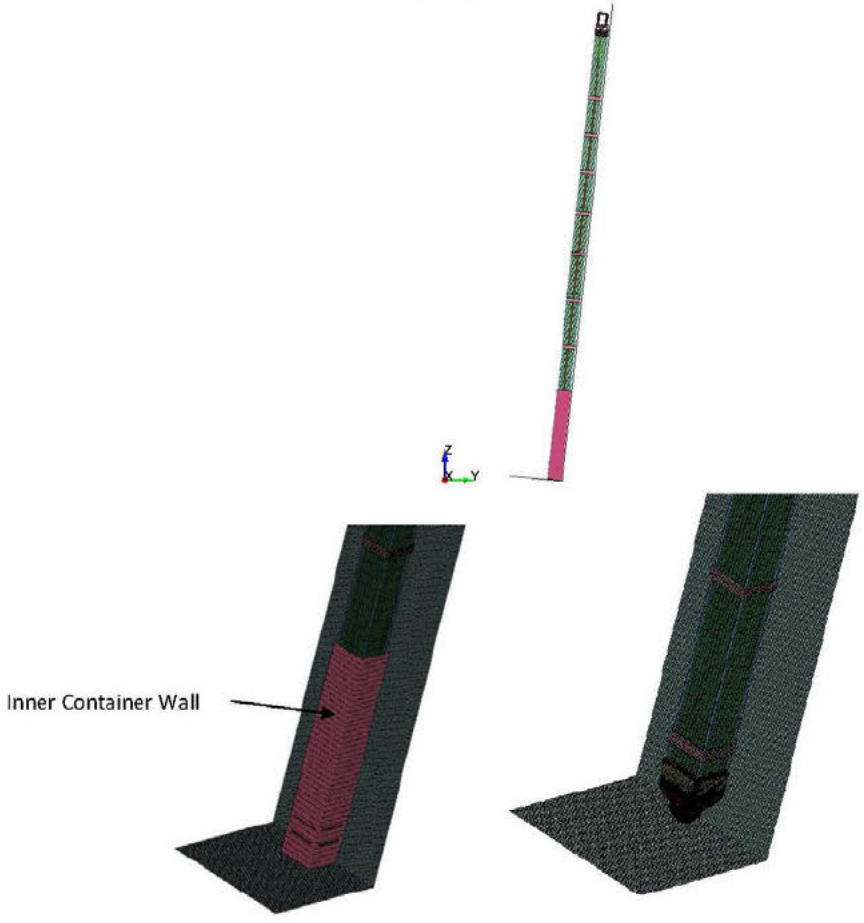

Figure 7.7.3.1-1: Model Set-Up - CG over Corner Drop - Cold Condition

[redacted]

The deformed shape of the fuel bundle under side drop cold condition is shown in Figure 7.7.3.1-2. As can be seen, the lower end of the fuel bundle suffers some damage but the cladding tubes maintain their integrity. The cladding tubes bend and some of them slip out of the lower tie plate support at the bottom. The top cage at the top, supporting the cladding tubes also slides away but still keeps the tubes in place.

Figure 7.7.3.1-2: Deformed Shape - CG Over Corner Drop - Cold Condition

Form NSA-EN-13-03 R1

[redacted]

7.7.3.2 Hot Condition - Case 3B

The model set up for the CG over corner drop hot condition is shown in Figure 7.7.3.2-1. The fuel bundle is inclined about 6 deg with vertical. The surface on which the fuel bundle is dropped is assumed to be rigid. Use of rigid surface results in conservative deformation/ damage to the fuel bundle and the predicted response is very conservative. Also the lower portion of the fuel bundle is covered by a thin sheet of SS304L sheet representing a portion of the walls of the inner container.

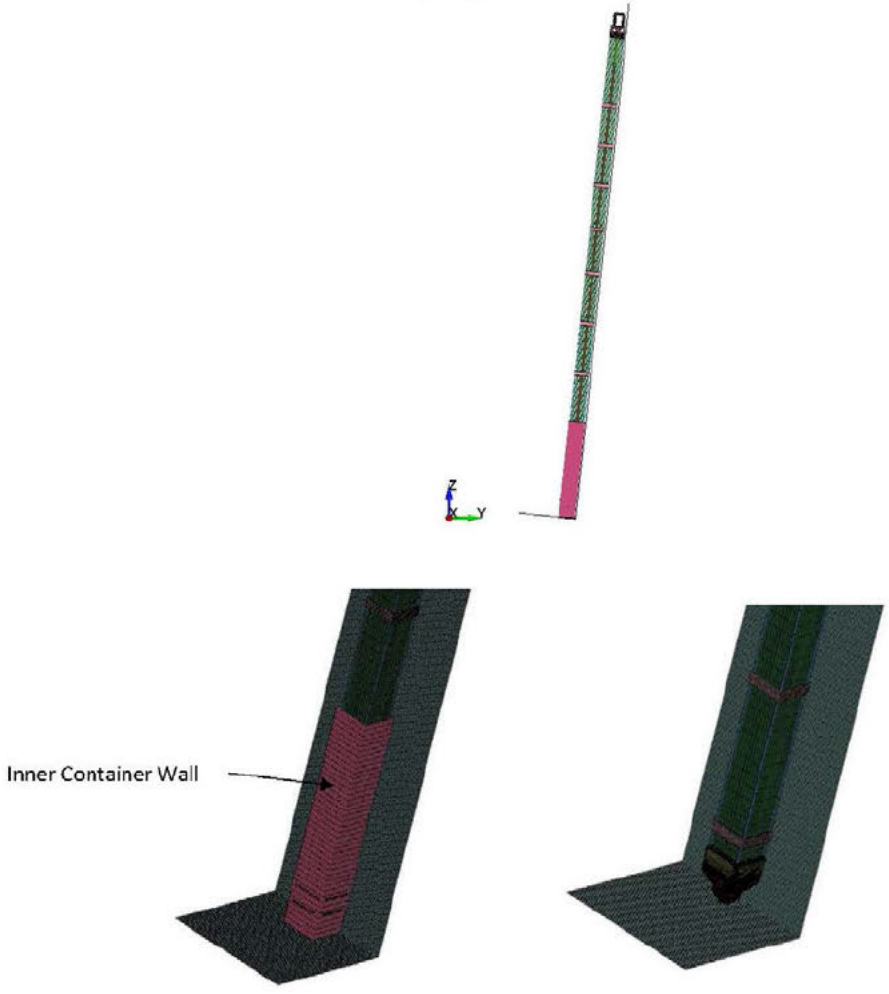

Figure 7.7.3.2-1: Model Set-UP - CG Over Corner Drop Hot Condition

Form NSA-EN-13-03 R1

[redacted]

The deformed shape of the fuel bundle under side drop hot condition is shown in Figure 7.7.3.2-2. As can be seen, the lower end of the fuel bundle suffers damage but the cladding tubes maintain their integrity. The cladding tubes bend and some of them slip out of the lower tie plate support at the bottom. The top cage at the top, supporting the cladding tubes also slides away but still keeps the tubes in place. The fuel is contained inside and is not exposed.

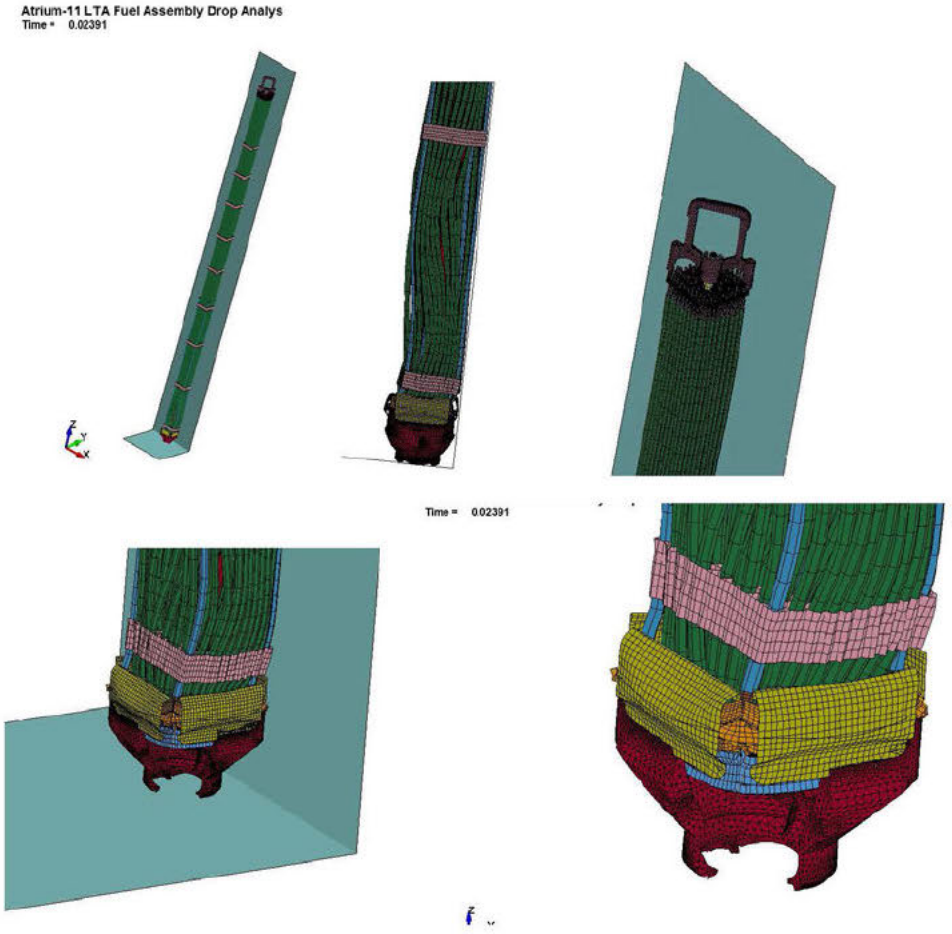

Figure 7.7.3.2-2: Deformed Shape - CG Over Corner Drop - Hot Condition

Form NSA-EN-13-03 R1

[redacted]

7.8 COMPARISON WITH DROP TEST RESULTS

7.8.1 Side Drop

The Certified Test Unit CTU 1 in Ref. 18 was dropped 30-ft with a slap-down on the lid. The damage to the fuel is described as minimum damage to the fuel assemblies. Some twist to the bundle was shown with minimal damage to the fuel rods. The damage to the fuel bundle is shown in the photo of Figure 7.8.1-1 below. The finite element simulation result presented in Section 7.7.1 and also shown in Figure 7.8.1-2 shows more damage than the actual test result. Therefore, the dynamic simulation is conservative.

Figure 7.8.1-1 Fuel Damage during a Slap-Down Drop

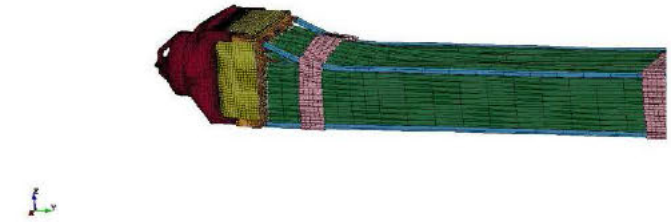

Figure 7.8.1-2 Fuel Damage during a Slap-Down Drop - Finite Element Analysis

[redacted]

7.8.2 Bottom End Drop

The Certified Test Unit CTU 2 in Ref. 18 was dropped 30-ft with its bottom end down. The damage to the wood is described as major crushing of the wood at the end of the inner package and breaking of the inner wall of the inner container on the impacted end. The damage to the fuel is described as fuel was bent and separated from end fittings. Fuel spacers were damaged. Fuel rods had no significant damage. Fuel bending was evident. The damage to the fuel is shown in the photo of Figure 7.8.2-1 below. The finite element simulation result presented in Section 7.7.2 and also shown in Figure 7.8.2-2 shows more damage than the actual test result. Therefore, the dynamic simulation is conservative.

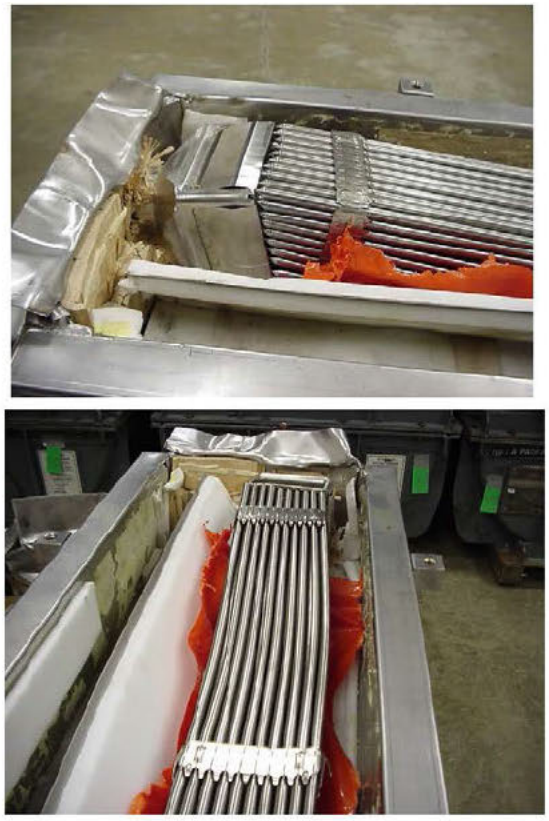

Figure 7.8.2-1 Actual Fuel Damage during a Bottom End Drop Event

ATKINS-NS-DAC-AREVA-14-01 (NSA-DAC-AREVA-14-01)
Rev. 1
Page 45 of 55

[redacted]

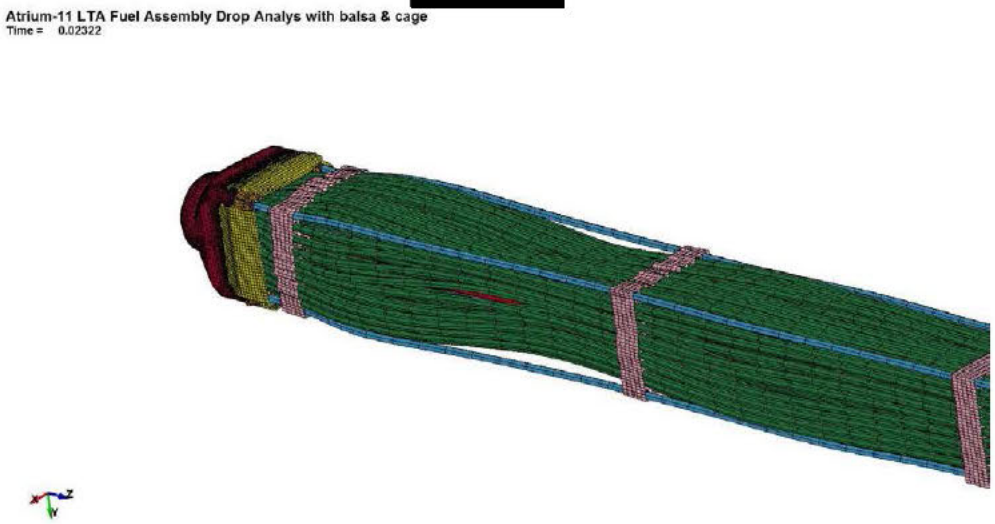

Figure 7.8.2-2 Fuel Damage during a Bottom End Drop Event - Finite Element Analysis

Form NSA-EN-13-03 R1

[redacted]

7.9 Fuel Rod Pitch Change

[redacted]

The drop case with the worst fuel rod deformation is Case 2B, bottom end drop under hot condition. The maximum deformation at the bottom section of the fuel bundle is shown in Figure 7.9-2 below. The cross-section A-A is selected by visual inspection of the results. An exhausted search of all cross-sections along the longitudinal direction for maximum pitch change between fuel rods is not performed.

[redacted]

Form NSA-EN-13-03 R1

Since the deformation is almost symmetrical in both in X and Y-direction, a quarter of the fuel rods are selected to check the pitch change between the fuel rods. The fuel rods selected for pitch check is shown in Figure 7.9-3 below.

[redacted]

[redacted]

A typical time history of pitch change for fuel rods between rod position A1 and rod position A2 is shown in Figure 7.9-4 below. The pitch value represents the resultant value in the horizontal (XY) plane.

[redacted]

This Section is updated in Rev. 1 to match the post processing methodology for calculating the pitch change as reported in Appendix C. Appendix C utilizes a modified finite element model of the fuel rod and pellet where the fuel pellet mass and the cladding are decoupled to provide an improved estimate of the rod pitch change.

[redacted]

Table 7.9-1 Pitch Change between Fuel Rods Oriented Along X-Direction.

[redacted]

Form NSA-EN-13-03 R1

[redacted]

Table 7.9-2 Pitch Change between Fuel Rods Oriented Along Y-Direction.

[redacted]

Form NSA-EN-13-03 R1

[redacted]

7.10 Fuel Bundle Overall Dimension Change

Section maps along the cross-section A-A of the fuel bundle array are shown in Figure 7.10-1 below. This cross-section corresponds to Section B-B in Figure 7.9-2. The section maps are utilized to evaluate the outside dimension changes of the fuel rod boundary after the end drop impact.

The changes in outside dimensions between fuel rods of the outer rows or columns are presented in Table 7.10-1 as follows. Note that the dimensions are measured from centerline of the cladding thickness.

[redacted]

Form NSA-EN-13-03 R1

[redacted]

Form NSA-EN-13-03 R1

[redacted]

Form NSA-EN-13-03 R1

[redacted]

8. REFERENCES

1 NRC Regulations 10 CFR, Part 71-Packaging and Transportation of Radioactive Material. 71.71 Normal Condition of Transport.
2 NRC Regulations 10 CFR, Part 71-Packaging and Transportation of Radioactive Material. 71.73 Hypothetical Accident Condition.
3 AREVA A1C-813768 Rev. 1
4 Global Nuclear Fuel – Japan (fka Japan Nuclear Fuel Co. Ltd). Application for Approval of Packaging, Type RAJ-II. Sto-M00-034, dated September 26, 2000
5 LS-DYNA Version 971 R5.1, Livermore Software Technology Corporation.
6 NSA_TR_12_01_R0, "LSDYNA Verification on NSA Server", September 10, 2012
7 ASME Code 2010, Subsection III, Appendix F. Section F-1341.4
8 Outer Container Drawings

Drawing number	Number of sheets	Revision No.	Name
105E3737	7	1	Outer Container Assembly Licensing Drawings
105E3738	9	3	Outer Container Main Body Assembly Licensing Drawings
105E3739	5	1	Outer Container Fixture Assembly Licensing Drawings
105E3740	5	1	Outer Container Fixture Assembly Installation Licensing Drawings
105E3741	2	1	Outer Container Shock Absorber Assembly Licensing Drawings
105E3742	4	1	Outer Container Bolster Assembly Licensing Drawings
105E3743	6	1	Outer Container Lid Assembly Licensing Drawings
105E3745	9	4	Inner Container Main Body Assembly Licensing Drawings
105E3746	2	1	Inner Container Parts Assembly Licensing Drawings
105E3747	5	1	Inner Container Lid Assembly Licensing Drawings
105E3748	3	1	Inner Container End Lid Assembly Licensing Drawings
105E3773	1	1	Protective Case

9 AREVA Design Specification 08-5053504-001 LTP-2 Tubing with Fe-Enhanced Liner for Fuel Rod Cladding.
10 ASME B&PV Code, 2010, Section VIII, Div 2, Annex 3.D
11 "Review of Zircaloy-2 and Zircaloy-4 properties Relevant to N.S. Savannah Reactor Design" C.L. Whit Marsh, ORNL-3181, July 9, 1962.
12 Measurements_Of_Elastic_Modulus_In_Zr_Alloys_For_CANDU_Applications, Pan, Wang and He, AECL, 11th International Conference on CANDU Fuel, Ontario, Canada, 2010, October CW-128700CONF-001
13 ASME B&PV Code, 2010, Section II, Part D
14 ASME New Section III Appendices, Appendix I Article A-1250, August 7, 2012 Record 09-2216
15 "Impact tensile testing of stainless steels at various temperatures" D.K. Morton and R. K. Blandford, March 2008, INL/EXT-08-14082
16 Hoadley, R. Bruce, "Understanding Wood: A Craftsman's Guide to Wood Technology", ISBN 1-56158-358-8, The Taunton Press, Inc., Newtown, CT, 2000
17 GNF RAJ-II Licensing Application, SAR, Rev.8, September 2013, pending NRC Approval.
18 GNF RAJ-II Licensing Application, SAR, Rev.7
19 ASME Code 2010, Subsection III, Appendix F. Section F-1341.4
20 AREVA Drawings FS1-0011525 R1, FS1-0012534 R1, FS1-0012535 R1
21 "TDR-ATRIUM 11 Lead Test Assemblies Design & Licensing Overview Report (LTAOR), AREVA Report FS1-0012986, Rev.1

Form NSA-EN-13-03 R1

[redacted]

Appendix A
Normal and Accident Conditions of Transport

1 Normal Conditions of Transport

1.1 Thermal

For the cold condition, an ambient temperature of -40°C is used in the evaluation as specified in 10 CFR 71.71(c) (2). During normal conditions of transport, there is negligible heat generated in the fuel, and this cold condition temperature can be assumed to be uniform throughout the total package of the TN-B1/RAJ-II container with the ATRIUM 11 fuel.

For the hot condition, 10 CFR 71.71 (d) (3) (1) specifies an ambient temperature of 38°C in direct sunlight with a total insolation of 800 g cal/cm^2 during a twelve hour period. Using these inputs and neglecting any decay heat in the fuel, the analysis results presented in Reference 18 computes a maximum package temperature of 77°C. The results of the referenced thermal analysis depend only on the design details of the RAJ-II container, and not on the ATRIUM 10 fuel contents. These analysis results with a maximum package temperature of 77°C are also applicable to the ATRIUM 11 fuel in the identical TN-B1/RAJ-II container. This maximum temperature occurs on the package exterior.

1.1.1 Differential Thermal Expansion

For both the cold and hot conditions, a uniform temperature for the complete fuel assembly is assumed. The maximum temperature computed for hot conditions on the package exterior is conservatively assumed for the fuel. Although at the same temperature, the different material properties of the fuel pellets and cladding result in changes in the relative dimensions between components at the cold and hot conditions due to differential thermal expansion.

Considering thermal expansion in the radial direction, the relevant nominal dimensions at a room temperature of 20°C are:

[redacted]

The nominal diametral clearance at room temperature between the OD of the fuel and the ID of the cladding is therefore,

[redacted]

For the fuel pellet, the strain due to contraction or expansion from the temperature change is,

$$\varepsilon_{fuel} = \left(\frac{\Delta D}{D}\right)_{fuel} = -3.28\text{x}10^{-3} + 1.179\text{x}10^{-5}\,T - 2.429\text{x}10^{-9}\,T^2 + 1.219\text{X}10^{-12}\,T^3 \quad \text{(Ref. 1)}$$

where the temperature, T, is the final temperature in degrees Kelvin, K.

[redacted] The coefficient of thermal expansion for the zirconium cladding is 7.4×10^{-6} in/in/°C. The strain due to contraction or expansion is,

$$\varepsilon_{clad} = \left(\frac{\Delta D}{D}\right)_{clad} = 7.4 \times 10^{-6} (\Delta T) \qquad \text{(Ref. 1)}$$

The cold and hot conditions to be considered are -40°C and 77°C. In the radial direction, the change in the clearance between the outside diameter of the fuel pellet and the inside diameter of the cladding is computed in the tables below.

Table 1-1. Thermal Expansion, Cold conditions, -40°C, ΔT = -60°C, T = 233°K

	Strain	Diameter change, ΔD, inch	Final Diameter, inch
Fuel Pellet	-6.49×10^{-4}	$\varepsilon_{fuel} \times D_{fuel} = -2.07 \times 10^{-4}$	[redacted]
Cladding	-4.44×10^{-4}	$\varepsilon_{clad} \times D_{clad} = -1.44 \times 10^{-4}$	
Net diametral clearance, inch			

Table 1-2. Thermal Expansion, Hot conditions, 77°C, ΔT = 57°C, T = 350°K

	Strain	Diameter change, ΔD, inch	Final Diameter, inch
Fuel Pellet	6.01×10^{-4}	$\varepsilon_{fuel} \times D_{fuel} = 1.92 \times 10^{-4}$	[redacted]
Cladding	4.22×10^{-4}	$\varepsilon_{clad} \times D_{clad} = 1.37 \times 10^{-4}$	
Net diametral clearance, inch			

At both the cold and hot temperature conditions a clearance still exists between the fuel pellet OD and cladding ID.

1.1.2 Maximum Pressure

During fabrication, the fuel rods are pressurized to a [redacted] with helium prior to sealing. Using the ideal gas law, the fuel rod maximum internal pressure, P_{max}, at the calculated maximum normal temperature of 77°C is,

[redacted]

Subtracting atmospheric pressure this gives an applied load to the inside of the fuel rods [redacted]

1.1.3 Thermal Stresses

No stresses are generated in the cladding due to radial differential thermal expansion with the fuel pellets as a clearance still exists between the pellet OD and cladding ID. Stresses due to differential thermal expansion in the axial direction are negligible due to the design feature of the fuel rod assembly that preloads the fuel pellets in the fuel rod and allows for relative axial movement of the fuel within the cladding. Also, the fuel rods are allowed to expand axially, and no significant thermal stresses due to axial differential thermal expansion are generated within the fuel assembly. The tangential stress, σ_t, in the fuel rod due to an internal pressure [redacted]

[redacted]

Where,

P = internal pressure, psi
r = cladding outside radius, in
t = cladding radial thickness, in

The fuel temperature and pressure at the normal condition of transport are well below those at normal operating conditions within the reactor.

1.2 Reduced External Pressure

Since the TN-B1/RAJ-II container does not have a pressure tight seal, a change in the external pressure of the container can be assumed to be experienced by the internal fuel assembly. The effect of a reduced external pressure of 3.5 psia identified in CFR 71.71 (c) (3) will give an increase the tangential stress, $\Delta\sigma_t$, in the fuel rod due to the corresponding increase in internal pressure by,

$$\Delta\sigma_t = \frac{\Delta P\, r}{t} = \frac{3.5 \times 0.1851}{0.02245} = 29 \text{ psi}$$

Where,

ΔP = increase in internal pressure, psi
r = cladding outside radius, in
t = cladding radial thickness, in

This stress increase is negligible on the fuel tube compared to the increase in stresses experienced during normal operating conditions within the reactor pressure.

1.3 Increased External Pressure

The fuel rods are pressurized to a maximum [redacted] with helium prior to sealing. The effect of an increased external pressure of 20.0 psia identified in CFR 71.71 (c) (4) is to decrease the effective internal pressure and therefore the tangential stress, $\Delta\sigma_t$, in the fuel rod due by,

$$\Delta\sigma_t = \frac{\Delta P\, r}{t} = \frac{20 \times 0.1851}{0.02245} = 165 \text{ psi}$$

Where,

ΔP = increase in internal pressure, psi
r = cladding outside radius, in
t = cladding radial thickness, in

In addition, due to the small clearance between the outside diameter of the fuel pellets and the inside diameter of the cladding, the fuel pellets within a fuel tube will prevent any radial buckling failure of the tube due to a relatively large increase in the external pressure.

1.4 Vibration

[redacted]

The ATRIUM 11 fuel will be transported within the same packing as the ATRIUM 10 fuel, using the same cushioning material and vibration isolation system. The design of this system prevents any significant vibratory stresses as discussed in Reference 18. Vibration normally associated with transportation as identified in 10 CFR 71.71 (c) (5) will have negligible effect on the fuel assembly structure.

1.5 Water Spray

The fuel tubes are not affected by water spray on the exterior surface of the TN-B1/RAJ-II container identified in 10 CFD 71.7 (c) (6).

1.6 Penetration

Results of prior drop testing of the TN-B1/RAJ-II container with ATRIUM 10 fuel from a height of 40 inches on to a puncture bar showed no penetration of the outer container (Ref. 1). The kinetic energy associated with this drop is significantly higher and bounding compared to a 40 inch drop of a 13 pound steel cylinder as specified for the penetration requirement in CFR 71.71 (c) (10). Since the ATRIUM 11 will be transported in the same identical TN-B1/RAG-II container, a drop of the 13 pound puncture bar will not penetrate the outer container and cause any damage to the fuel assembly.

1.7 Compression

The weights of the ATRIUM 10 and ATRIUM 11 fuel assemblies are essentially identical. The weight of the package consisting of the TN-B1/RAJ-II container and either fuel assembly is less than 11,000 pounds, and the requirement in 10 CFR 71.71 (c) (9) is that the package must support five times its weight without damage. The TN-B1/RAJ-II container with the ATRIUM 10 fuel has been shown to meet the compression requirement (Ref. 1). As the compression loading of the TN-B1/RAJ-II container with the ATRIUM 11 fuel will be the same, the TN-B1/RAJ-II and ATRIUM 11 package also meets the compression loading requirement.

1.8 Free Drop

The TN-B1/RAJ-II container at maximum payload weight with the ATRIUM 11 fuel is less than 11,000 pounds, and a four foot drop of the package is required per 10 CFR 71.71 (c) (7). Damage from this drop is significantly bounded by the 30 foot drop accident requirement specified in CFR 71.73 (c) (1).

Four foot drop testing results of the RAJ-II package with ATRIUM 10 fuel has been performed As discussed Reference 18, this testing demonstrated that the resulting damage had no effect on the containment or the ability to meet the requirements of 10 CFR 71.

The ATRIUM 10 and ATRIUM 11 fuel assemblies have essentially the same weight. In addition, identical materials and manufacturing processes are used in the fabrication of these fuels. Analysis results are presented in section 3.0 for the 30 foot accident drop of the ATRIUM 11 fuel assembly. As discussed, these results show that the calculated overall behavior and damage to the fuel assembly is similar to that observed during 30 foot drop testing of the RAG-II package with the ATRIUM 10 fuel (Ref. 1). For these reasons, it can be concluded that the behavior and damage to the ATRIUM 11 fuel assembly within the same TN-B1/RAJ-II container during the four foot drop will be similar to that observed for the ATRIUM 10 fuel during the four foot drop test, and the requirements for 10 CFR 71.71 (c) 7 are also met.

[redacted]

1.9 Corner Drop

The corner drop requirement of 10 CFR 71.71 (c) (8) does not apply as the complete TN-B1/RAJ-II package weight with the Atrium 11 fuel exceeds 220 pounds.

2.0 Accident Conditions of Transport

2.1 Crush

The TN-B1/RAJ-II package weight with either one or two ATRIUM 11 fuel assemblies as contents exceeds 1,100 pounds, and the dynamic crush requirement of 10 CFR 71.73 (c) (2) is not applicable.

2.2 Puncture

Prior drop testing of the TN-B1/RAJ-II container with the ATRIUM 10 fuel from a height of 40 inches on to a puncture bar did not penetrate the outer container (documented in Reference 4). The maximum payload weight of the package was used in these tests. The same TN-B1/RAJ-II container will be used for the ATRIUM 11 fuel, and as the difference in weight between the ATRIUM 10 and ATRIUM 11 fuel contents is negligible, the kinetic energy associated with the drop will be the same for the packages with the two different fuels. Any change in damage to the outer container, and therefore the fuel assemblies, will also be negligible with the ATRIUM 11 payload compared to the ATRIUM 10 fuel, with no penetration of the fuel rods. The requirement of 10 CFR 71.73 (c) (3) is met.

2.3 Thermal

The hot accident condition specified in 10 CFR 71.73 (d) (4) that the package be subjected to a fully engulfed fire with flame temperature of at least 800°C for a period of 30 minutes. A transient finite element analysis is summarized in Reference 18 that was performed to simulate the fire event on the RAJ-II package with the ATRIUM 10 fuel. The analysis conservatively ignores the outer container, and only the inner container is included in the model. The fuel assembly itself within the container is also not considered, and therefore this analysis of the hot accident condition is also applicable to the TN-B1/RAJ-II container to be used with the ATRIUM 11 fuel.

The maximum fuel rod temperature is conservatively assumed to be the same as the container inner wall temperature of 648°C that was calculated during the transient thermal analysis. A bounding temperature of 800°C is assumed in the evaluation.

2.3.1 Differential Thermal Expansion

For the thermal accident condition, the fuel pellets and cladding are conservatively assumed to be at the same bounding temperature of 800°C. The different material properties of these components result in changes in the relative dimensions from room temperature due to differential thermal expansion.

Considering thermal expansion in the radial direction, the relevant nominal dimensions at a room temperature of 20 °C are:

[redacted]

The nominal diametral clearance at room temperature between the OD of the fuel and the ID of the cladding is therefore

[redacted]

For the fuel pellet, the strain due to contraction or expansion from the temperature change is,

$$\varepsilon_{fuel} = \left(\frac{\Delta D}{D}\right)_{fuel} = -3.28\text{x}10^{-3} + 1.179\text{x}10^{-5}\,T - 2.429\text{x}10^{-9}\,T^2 + 1.219\text{X}10^{-12}\,T^3 \quad \text{(Ref. 1)}$$

where the temperature, T, is the final temperature in degrees Kelvin, K.

The coefficient of thermal expansion for the zirconium cladding is $7.4\text{x}10^{-6}$ in/in/°C. The strain due to contraction or expansion is,

$$\varepsilon_{clad} = \left(\frac{\Delta D}{D}\right)_{clad} = 7.4\text{x}10^{-6}\,(\Delta T) \qquad \text{(Ref. 1)}$$

In the radial direction, the change in the clearance between the outside diameter of the fuel pellet and the inside diameter of the cladding at the maximum temperature of 800°C is computed as follows.

Table 2-1. Thermal Expansion, Accident Hot conditions, 800°C, ΔT = 780°C, T = 1073°K

	Strain	Diameter change, ΔD, inch	Final Diameter, inch
Fuel Pellet	8.08×10^{-3}	$\varepsilon_{fuel} \times D_{fuel} = 2.58 \times 10^{-3}$	[redacted]
Cladding	5.77×10^{-3}	$\varepsilon_{clad} \times D_{clad} = 1.88 \times 10^{-3}$	
Net diametral clearance, inch			

A clearance still exists between the fuel OD and cladding ID for the thermal accident condition.

2.3.2 Maximum Pressure

The fuel rods are pressurized to a maximum [redacted] with helium prior to sealing. Using the ideal gas law, the fuel rod maximum internal pressure, P_{max}, at the bounding maximum temperature of 800°C is,

[redacted]

Subtracting atmospheric pressure, this gives an applied load to the inside of the fuel rods of 332.1 psi.

2.3.3 Thermal Stresses

[redacted]

No stresses are generated in the cladding due to radial differential thermal expansion with the fuel pellets as a clearance still exists between the pellet OD and cladding ID. Stresses due to differential thermal expansion in the axial direction are negligible due to the design feature of the fuel rod assembly that preloads the fuel pellets in the fuel rod and allows for relative axial movement of the fuel within the cladding. Also, the fuel rods are allowed to expand axially, and no significant thermal stresses due to axial differential thermal expansion are generated within the fuel assembly. The tangential stress, σ_t, in the fuel

[redacted]

Where,

P = internal pressure, psi
r = cladding outside radius, in
t = cladding radial thickness, in

As noted in Reference 18, it has been demonstrated by testing that fuel rods with similar cladding material can withstand temperatures of excess of 800°C for more than 60 minutes without failure. In these tests, the fuel was pressurized with 10 atmospheres of helium during fabrication and resulting in an internal pressure at 800°C of,

$$P_{max} = 161.7 \text{ x} \left(\frac{273 + 800}{273 + 20} \right) = 592.2 \text{ psia}$$

This gives an applied load to the inside of the test fuel rods of 577.5 psi and a corresponding tangential stress of 4510 psi. This stress is higher than that calculated in the ATRIUM 11 fuel during the hot accident condition by a factor of [redacted] = 1.65, which shows significant margin against failure.

2.4 Immersion – Fissile Material

The requirement of 10 CFR 71.73 (c) (5) is related to the criticality of the TN-B1/RAJ-II package, and is addressed in the criticality evaluation.

2.5 Immersion – All Packages

The TN-B1/RAJ-II package is not sealed against pressure, and therefore the fuel rods will be subject to an external pressure generated by the water immersion load defined in 10 CFR 71.73 (c) (6). This load is equivalent to a 50 ft head of water (or 21.7 psi). However, immersion is a normal design condition for the fuel tubes which are designed to withstand a pressure differential of greater than 1000 psi. The immersion load will have a negligible effect on the fuel assembly structural integrity.

[redacted]

Appendix B

Impact of Shipping Fuel Assemblies with Reduced Weight in the RAJ-II Container

B1. Introduction and Summary

The total weight of the RAJ-II container with the mock-up fuel ballasts used in the drop test [Ref. 4] is 3285 lb (1490 kg). The weight of the ballast simulating the two fuel bundle is 560 kg. The weight of the RAJ-II container is 2050 lbs (1490 kg-560 kg=930 kg). It is based on the assumption that the RAJ-II container is fully loaded that the LSDYNA simulation of the accident drops of the fuel bundle is performed as reported in the main report. When the RAJ-II container holds reduced weight, the dynamic behavior of the shipping container is altered and the impact on peak acceleration is determined and reported in this appendix. Since the bottom end drop is the most critical drop, the change of peak acceleration during bottom end drop is evaluated.

The methodology to determine the peak acceleration for the reduced weight is outlined as follows.

1. Start from the recorded end drop acceleration time-history (ATH) reported in the Japanese drop test.
2. Digitally enhance the ATH to remove the anomalies so that after numerical integration against time the derived velocity approaches zero at end of the impact and displacement is continuous and monotonic.
3. Generate the force-displacement curve of the cushioning material. The displacement is taken from step 2 above. The force (F) is the product of the acceleration (A) and the total weight of the container (M=3285 lbs) that F=M×A.
4. Develop a simple LSDYNA model using a plate and a crushable foam block. The weight of the plate represents the total weight of the container and the fuel bundle. The crushable foam has the force-displacement characteristics matches with the force-displacement curve generated in step 3 above.
5. Perform a LSDYNA dynamic drop simulation. The initial velocity of 527.45 in/second is applied to the plate mass.
6. Confirm that the peak acceleration agrees with the peak acceleration of 303 G reported in the drop test performed by the Japanese RAJ-II container.
7. Using the same LSDYNA model, the weight of the plate mass is changed to 2699 lb (=2050 lb + 584 lb + 65 lb). The total weight represents the shipping container (2050 lb), one Atrium-11 fuel bundle and the cage assembly (65 lb). The resulted peak acceleration is the predicted increased peak acceleration due to shipping with reduced weight.

The predicted peak acceleration with reduced fuel bundle weight is 367G. The peak acceleration used in the end drop simulation with full fuel bundle weight is 424 G. The factor of safety against fuel bundle collapse is 424/367=1.15. The detailed methodology is presented in the following sections.

B.2 The Enhancement of the Acceleration Time History for the Bottom End Drop.

The original and enhanced acceleration time history is presented in Figure B.2-1 below. After integration of the ATH with respect to time, the velocity time history of the dropping plate mass is presented in Figure B.2-2 below. After integration of the velocity time history, the displacement time history of the dropping plate mass is presented in Figure B.2-3 below. The actual displacement is in the downward direction.

[redacted]

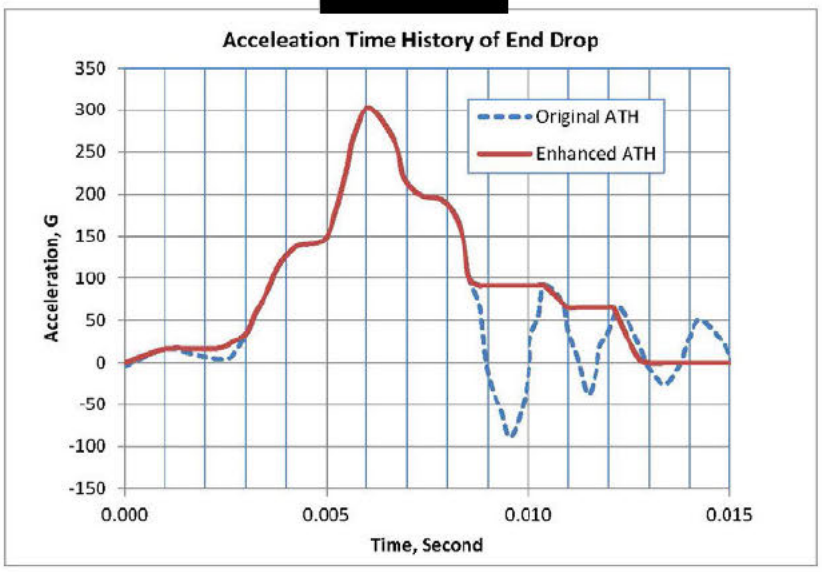

Figure B.2-1 Acceleration Time History

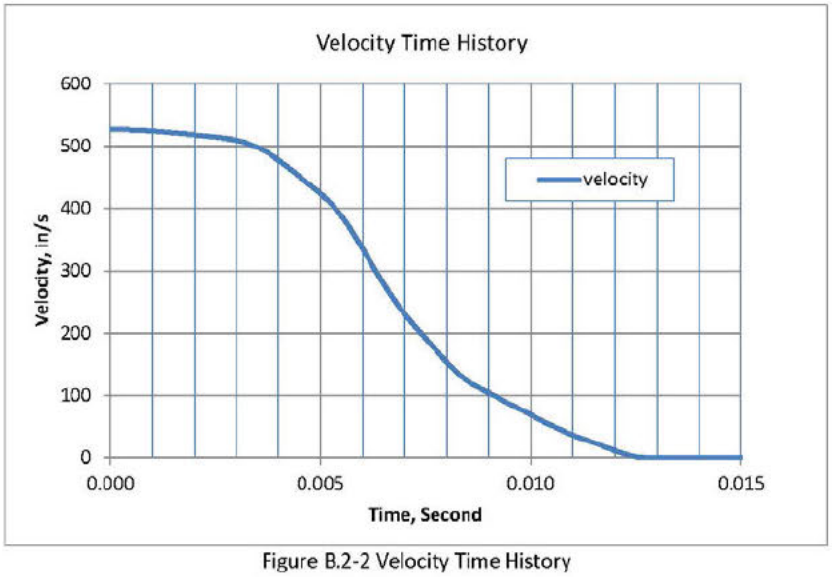

Figure B.2-2 Velocity Time History

[redacted]

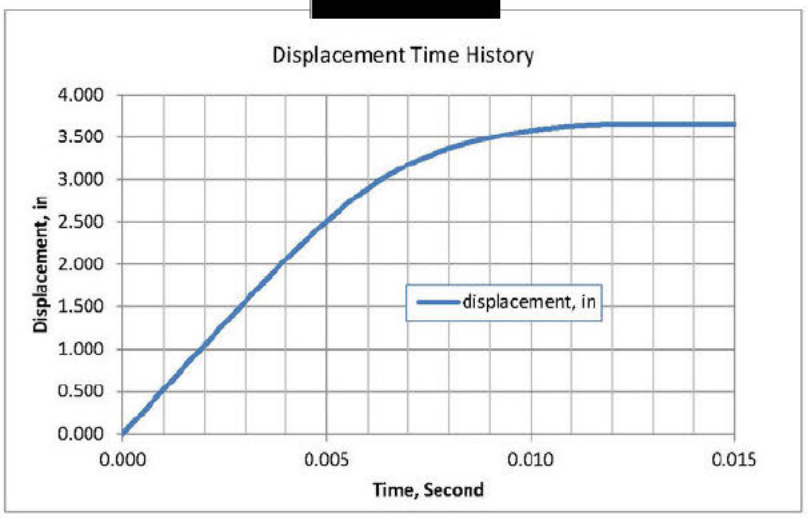

Figure B.2-3 Displacement Time History

B.3 The Force-Displacement Time History

The displacement is taken from Figure B.2-3 above. The force (F) is the product of the acceleration (A) in Figure B.2-1 and the total weight of the container (M=3285 lbs) that F=M×A. The force-displacement curve for the cushioning material at the bottom of the RAJ-II container is presented below.

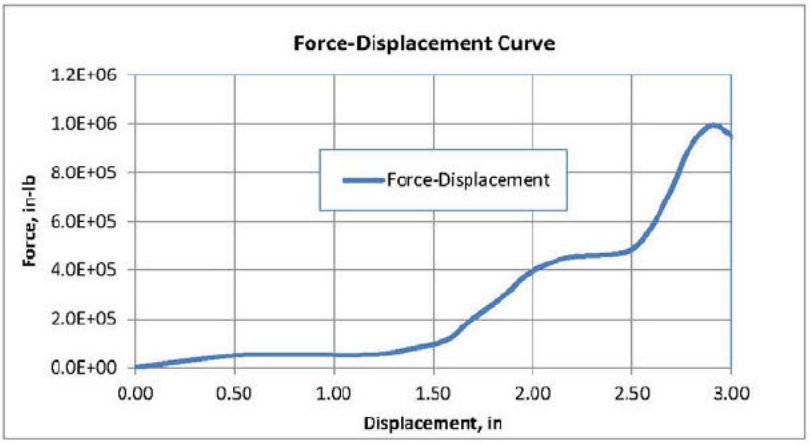

Figure B.3-1 Force-Displacement Curve of the Cushion Material

[redacted]

B.4 The LSDYNA Finite Element Model

The simplistic finite element model is shown in Figure B.4-1 below. The weight of the plate represents the total weight of the container and the fuel bundle (3285 lb). The crushable foam has the force-displacement characteristics matches with the force-displacement curve presented in Figure B.3-1.

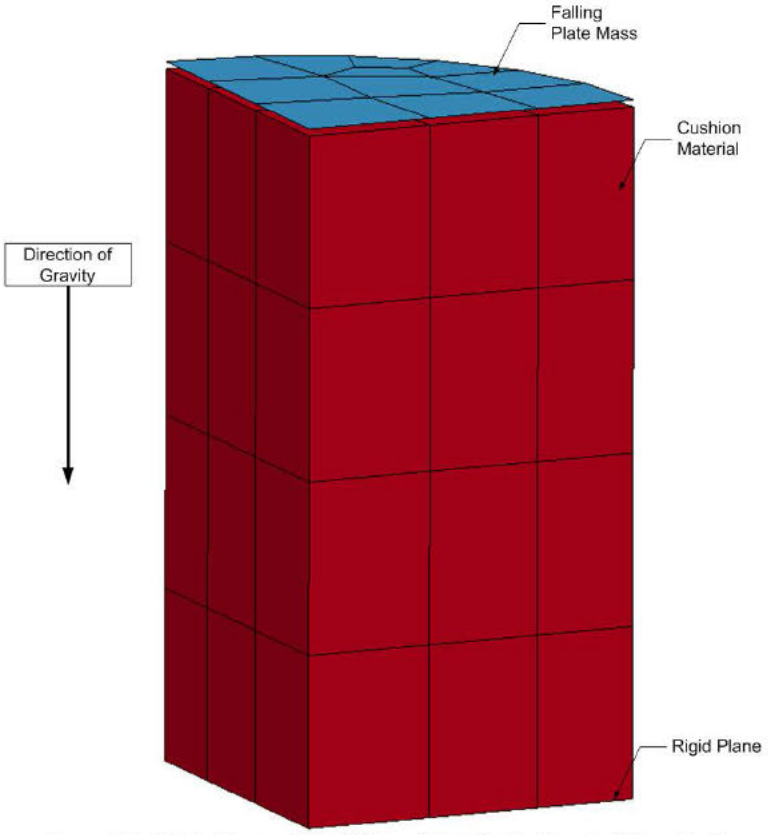

Figure B.4-1 Finite Element Model Simulating the Bottom End Drop Test

[redacted]

B.5 Dynamic Simulation of the Japanese Drop Test

To perform a LSDYNA dynamic drop simulation, the initial velocity of 527.45 in/second is applied to the plate mass. The resulted acceleration time history of the plate is filtered at 500 Hz. The acceleration time history of the plate mass is shown in Figure B.5-1 below. It agrees reasonably well with the peak acceleration of 303 G reported for the Certified Test Unit (CTU-1) in the drop test performed by the Japanese RAJ-II container. The result confirms that the material model is correct and the enhancement of the ATH is justified.

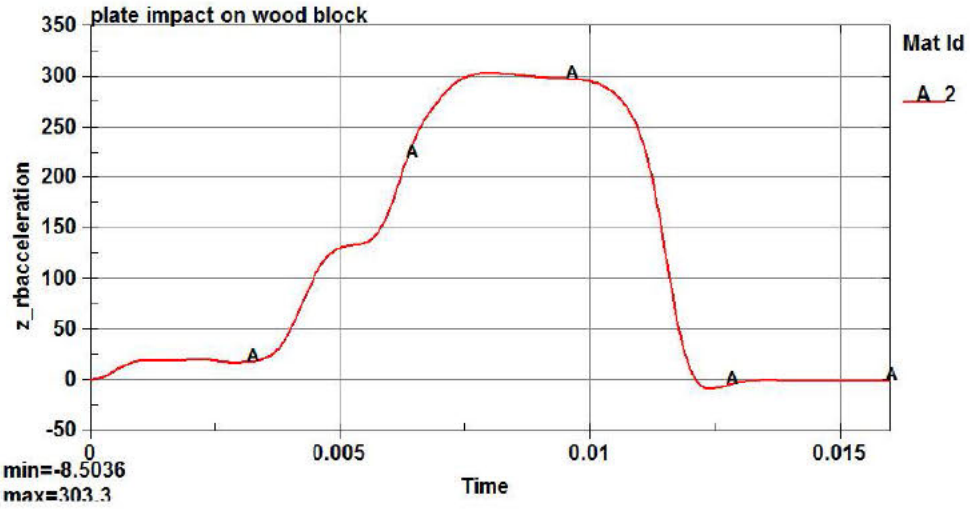

Figure B.5-1 Acceleration Time History of Simulated End Drop of Japanese CTU-1.

[redacted]

B.6 Dynamic Simulation of the Atrium-11 Shipping Configuration

Using the same LSDYNA model, the weight of the plate mass is changed to 2699 lb (=2050 lb + 584 lb + 65 lb). The total weight represents the shipping container (2050 lb), one Atrium-11 fuel bundle and the cage assembly (65 lb). The resulted peak acceleration is shown in Figure B.6-1 below. The predicted increased peak acceleration due to shipping with reduced weight is 367 G. The increase of peak acceleration is 21%.

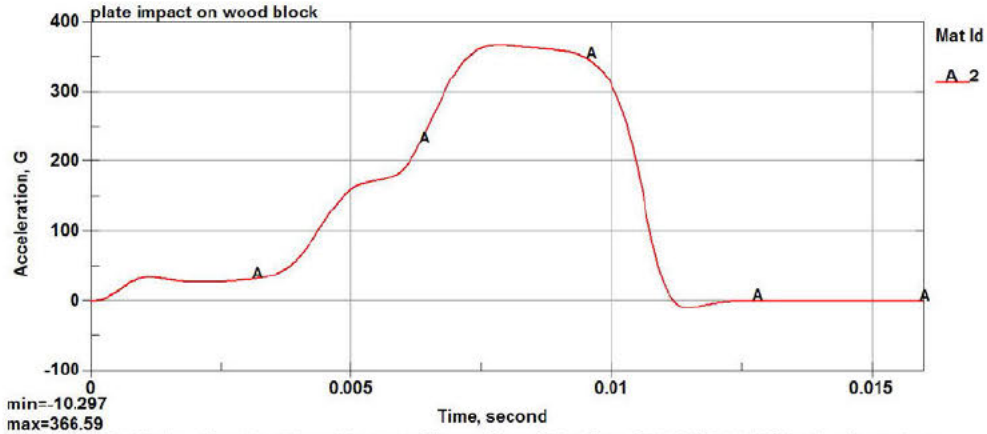

Figure B.6-1 Acceleration Time History of the reduced Weight of TN-B1/RAJ-II Shipping Container

B.7 Conclusion.

In the main report, the peak acceleration used in the end drop simulation is 424 G. Therefore, with the reduced weight in the shipping container, the factor of safety is 424/367=1.15. It is still safe to ship the single Atrium-11 fuel bundle in the TN-B1/RAJ-II container.

B.8 Future Work

In order to maintain a minimum factor of safety of 1.4 to guard against exceeding 70% of the plastic instability load, the end drop and corner drops may be analyzed with increase peak G loads by 21% to address the effects of reduced weight of payload in the TN-B1/RAJ-II container.

[redacted]

Appendix C

Pitch Changes of the Fuel Bundle After a 30-ft End Drop

C.1 Background

This DAC evaluates the fuel rod pitch change following a 30 foot end drop for two-element full region shipment for the ATRUIM 11 fuel elements.

Analyses presented in the main body of the report documented the structural analyses of the AREVA Atrium-11 LTA fuel assembly in the TN-B1 Container during Normal Condition of Transport (NCT) as per 10 CFR71.71 and Hypothetical Accident Transport Condition (HAC) of transport as per 10 CFR71.73.

The Analyses of the main body were simulated by the LSDYNA finite element dynamic simulation program with the accident time history (ATH) input derived from the actual drop test of RAJ-II (TN-B1) container (BSG-T98-005, Jan 1998) performed by Japan Nuclear Fuel Co., Ltd in the Licensing Application to Japan Science and Technology Agency. The peak values of ATH are scaled up from the actual drop test results to assure that a minimum factor of safety of 1.4 is maintained. Section 7.9 presents a set of values for the change in pitch for the ATRIUM-11 element for single element LTA shipments. For two-element full region shipments a more realistic best estimate evaluation is provided.

The finite element model employed in Section 7.9 assumed that the fuel pellet and the fuel cladding are coupled together such that the mass of the fuel pellets is uniformly distributed to the cladding surface. The lumping of the fuel mass in the cladding shell simplified the finite element development and reduced the computer run time. However, the model simplification made the cladding excessively heavy causing the fuel tube to buckle during and at the end of impact. This modeling approach is overly conservative when calculating the fuel tube pitch change. The model was modified to decouple the fuel pellets from the fuel cladding over the length of the fuel rod and lump the fuel pellet weight to the lower end of the fuel rod

The results in this Appendix do not change the overall analysis results presented in Section 7.9 and 7.10 of this DAC. However, the analysis presented in this appendix with the fuel mass decoupled from the cladding mass serves to improve the solution of the calculated fuel rod pitch changes that occur during a 30-ft end drop.

C.2 Purpose and Scope

The purpose of this analysis is to realistically assess the pitch change of the fuel rods considering the grouping effects of the fuel bundle and the individual lateral displacement of fuel rods as standalone single fuel rods.

The grouping effect of the fuel bundle is assessed using the same finite element model of the calculation described in section 7.1 with the exception that the fuel mass and fuel tube cladding are decoupled. The mass of the fuel pellet is lumped to the bottom end of the fuel tips therefore relieving the fuel cladding from the excessive weight of the fuel. The longitudinal inertia effect of the fuel pellet weight is still preserved in this modeling detail. However, the lateral inertia effect of

[redacted] the fuel pellet on the fuel cladding cannot be simulated by this simplistic modeling approach. Therefore a single rod finite element model is developed in Section C.6 to investigate the interaction between the fuel pellets and the fuel cladding during a vertical end drop impact event.

The fuel rod bundle model is 3-dimensional. During an end drop (along the Z-direction) scenario, the fuel rods buckle and move in the lateral direction (XY plane). When the fuel rod acts as a stand along vertical rod, the fuel rod may buckle in any direction in a random manner in the lateral plane. But as an individual rod among a group of vertical rods, the fuel rod is influenced by the behavior of the adjacent rods. This phenomenon is described as the grouping effect. It is not mathematically or kinematically constrained, but it is statistically observed in all similar physical natural phenomena. In the LSDYNA model, this phenomenon is achieved by applying an influence layer around each fuel tube such that the behavior of the fuel tube can influence the behavior of fuel tubes around it. The influence layer is implemented in the contact definition modeling of the fuel tubes.

The pitch change is calculated based on the lateral relative movement of two adjacent fuel tubes. The result of the pitch change is a collection of relative displacements for all adjacent fuel rods in the fuel bundle group. Since it is a collection of statistical samples, the result is best used by averaging all pitch changes. The averaged result of this modeling is used to compare with the calculated result of a single fuel rod model. The single-rod model consists of a single fuel rod (cladding), stacked fuel pellets and a rigid wall to apply the acceleration. The finite element model will be described in detail later.

The pitch change is presented as a percentage change of the final pitch between the original pitch of two adjacent fuel rods as specified in FS1-0012986 Rev. 1, Table 2-2. The final pitch is determined when the impact is over and the fuel rods are in steady state condition.

C.3 Description of the Fuel Bundle Model

The description of the fuel bundle is taken from Section 7.9 of main report and repeated as follows:

[redacted]

[redacted]

C.4 Pitch Change of Bundled Fuel Model

The pitch change results in the fuel bundle are reported at cross-section A-A shown in Figure C.4-1. By visual inspection of the analysis results, this section indicates the maximum lateral displacement of the fuel cladding at the bottom section of the fuel bundle.

[redacted]

As confirmed by Section C.5, the fuel rod pitch movements are almost symmetrical in both in X and Y-directions, and therefore a good assumption for evaluating the overall pitch changes between all fuel rods in the bundle is to use only the pitch changes computed for only a quarter of the fuel rods in the model. The fuel rods selected for the pitch change evaluation are shown in Figure C.4-2 below. The fuel rods in Column number A correspond to the fuel rods along the vertical center lines of the fuel bundle. The fuel rods in Row number 6 correspond to the fuel rods along the horizontal center lines of the fuel bundle. The placements of the fuel rods in the cross-sectional area in Figure C.3-1 are taken from the finite element model, which is developed based on the fuel bundle design drawings. The nominal pitches are specified in FS1-0012986, Rev. 1, Table 2-2, (Ref 21).

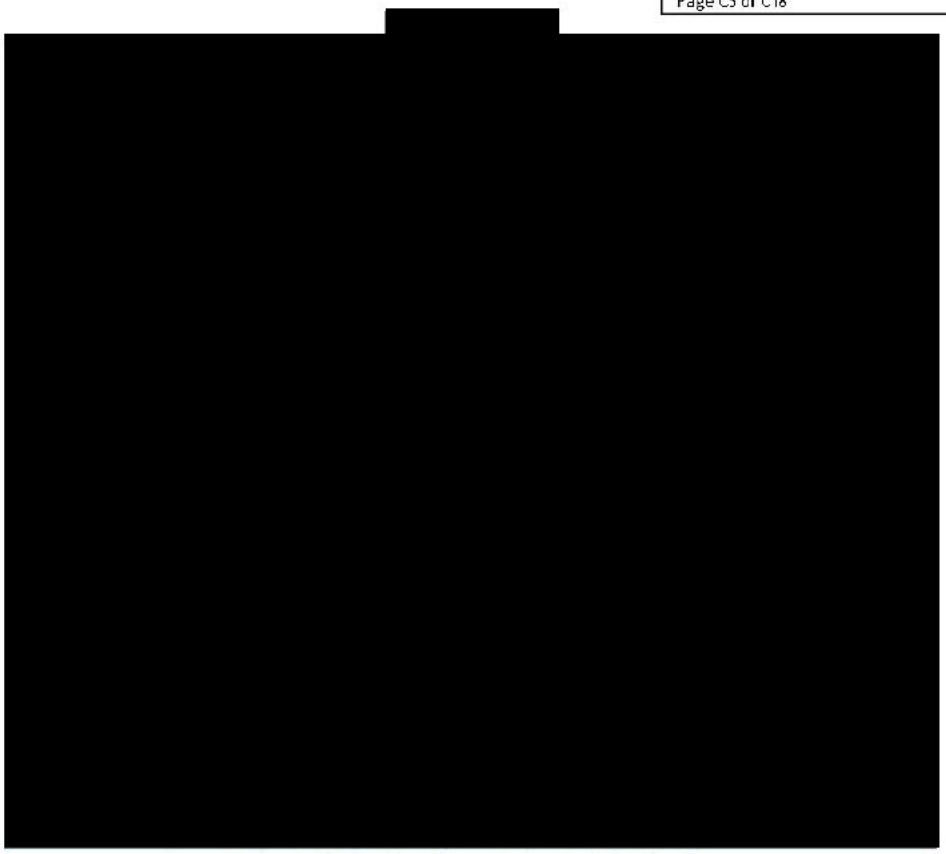

Figure C.4-2 Fuel Rod Map selected for Pitch Review

The fuel rod map, Figure C.4.2, is overlaid with column and row IDs to facilitate the identification of fuel rod locations in the array. The nodal points in the finite element model selected to report the pitch change are noted on the map. The calculated pitch change takes into account the X and Y-displacements (Δx and Δy) of the final position of each fuel rod after the end drop and represents the total change in distance between two adjacent fuel rods in the lateral plane. This is illustrated in Figure C.4-3. The pitch change between two adjacent fuel rods, Δp, is defined as a percentage by,

$$\Delta p = \frac{p_f - p_i}{p_i} \times 100$$

where

P_i = initial pitch between two adjacent fuel rods

P_f = final pitch between two adjacent fuel rods.

A typical time history of the pitch value for fuel rods between rod position A1 and rod position A2 is shown in Figure C.4-4. The net pitch change from the original value is shown in Figure C.4-5.

[redacted]

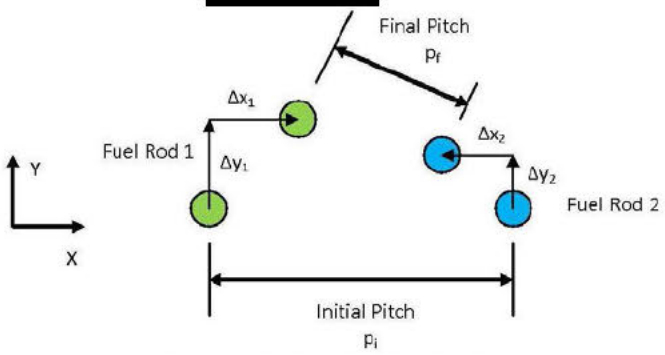

Figure C.4-3 Initial and Final Pitch Distance

[redacted]

Figure C.4-5 Net Pitch Change (P_f-P_i) Time History from the Original Value between Rod A1 and Rod A2.

The pitch changes after the bottom end drop between fuel rods oriented along the X-direction and between fuel rods oriented along the Y-direction are shown in Table C.4-1 and Table C.4-2 respectively, for convenience of listing the results. The first letter in the Rod Location ID represents the column or Row number. The second and third letters (or number) represent the row or column number in the array. For example Rod Position A23 means the pitch change between Fuel Rods in Column number A, position 2 and 3. Similarly, Rod Position 3AB identifies the pitch change between Rod in Row number 3, position A and B. A positive pitch change indicates an increase in pitch. A negative pitch change indicates a decrease in the pitch.

[redacted] Table C.4-1 Pitch Change between Fuel Rod Oriented Along the X-direction.

[redacted]

[redacted]

Table C.4-2 Pitch Change between Fuel Rods Oriented Along the Y-direction.

[redacted]

[redacted]

C. 5 Fuel Bundle Overall Dimension Change [redacted]

A typical deformed cross-section of the fuel bundle array after bottom end drop impact is shown in Figure C.5-1 below. This cross-section corresponds to Section A-A in Figure C.4-1. The cross-section before impact is shown in Figure C.3-1.

Figure C.5-1 Deformed Cross-Section of Fuel Bundle after Bottom End Drop

The changes in outside dimensions (OD) between fuel rods of the outer rows or columns are presented in Table C.5-1 below. Note that although the calculated dimensions are measured from centerline of the cladding thickness, these values are considered to be valid at the cladding outside diameter. The locations of the fuel rods selected for the pitch change reported are identified on the cross sections shown in Figure C.5-2 below. Note that the method for calculating the pitch change and average is the same as detailed in Section C.4.

Atkins-NS-DAC-AREVA-14-01 (NSA-DAC-AREVA-14-01, Rev. 1)
Rev. 1
Page C11 of C18

[redacted]

[redacted]

The average pitch change, p_{avg}, is calculated as,

$$P_{avg} = \frac{1}{m} \sum_{k=1}^{m} \Delta p_k$$

where m = number of pitch change entries in the table.

It can be observed from Table C.5-1 that

[redacted]

Atkins-NS-DAC-AREVA-14-01 (NSA-DAC-AREVA-14-01, Rev. 1)
Rev. 1
Page C13 of C18

[redacted]

[redacted]

C.6 Description of the Single Fuel Rod Model

The model consists of the single fuel rod (cladding), the dished fuel pellets (FS1-0012534 and FS1-0012535 [Ref. 20]), the cage spacer (FS1-0011525 [Ref. 20]), and the rigid wall to apply the acceleration. The finite element model is shown in Figure C.6-1 below. The dished fuel pellet is shown in Figure C.6-2 below.

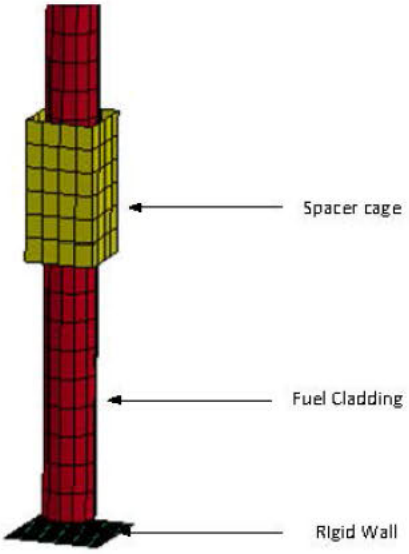

Figure C.6-1 Finite Element Model of a Single-Rod Fuel Tube.

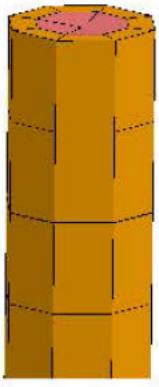

Figure C.6-2 Finite Element Model of the Dished Fuel Pellets.

[redacted]

The material properties of the finite element model are taken from the fuel bundle model used in Section 3. When inspecting fuel rod pitch changes in Section C.5, it is confirmed that during the end drop impact event, the fuel rods in the fuel bundle expand laterally in a symmetrical pattern both in the X and Y directions. The longitudinal geometric centerline of the fuel bundle and the cage spacer remain aligned with the direction of the end drop. Therefore, during the entire end drop event (less than 30 milliseconds), while the longitudinal movement of the cage spacer is less than 8-inches, the lateral positions of the cage spacers remains unchanged relative to the longitudinal centerlines of the fuel bundle. The buckling only occurs to the fuel tubes since the length to diameter ratio is very large. The lateral stiffness of the cage spacer shells to resist the lateral inertia force induced by the fuel tubes buckling is much greater than the lateral stiffness of the fuel tube. Therefore it is reasonable to assume that the boundary of the cage spacer is rigid relative to the flexibility of the fuel tube in the lateral direction. The cage spacer is therefore modeled as rigid at the lateral boundary to restrain its motion in the lateral plane (XY plane) and moves with the rigid wall in the vertical Z-direction. The restraint of the cage spacer in the vertical direction is conservative, since the vertical movement of the cage spacer tends to reduce the unsupported length of the fuel rod and increase the resistance to buckling. The gaps between the sides of the cage spacer and the fuel cladding are still elastic, reflecting that there are built-in spring clips on the cage spacer to support the fuel cladding laterally.

A uniform internal pressure of 94.7 psi is applied to the internal surface of the fuel cladding per Table 2-2 of FS1-0012986 Rev.1.0 [Ref. 21].

Boundary Conditions.

The acceleration applied to the single rod model through the rigid wall is taken from the output of the fuel tubes (Part 1) of Run Case HAC014-FA1 of the main calculation. The procedures to derive the acceleration are described as follows.

1. Obtain the rigid body Z acceleration output of finite element Part 3 (fuel tubes) from the MATSUM file. Integrate it to obtain the velocity time-history as shown in Figure below.

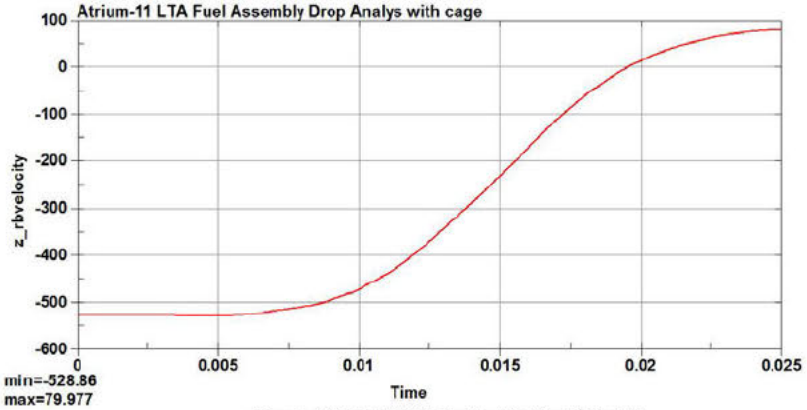

Figure C.6-3 Rigid Body Z-velocity of Part 3

2. Modify the acceleration curve at the time base so the integrated velocity time history at steady state is 0 (refer to Figure C.6-4 as shown below).

[redacted]

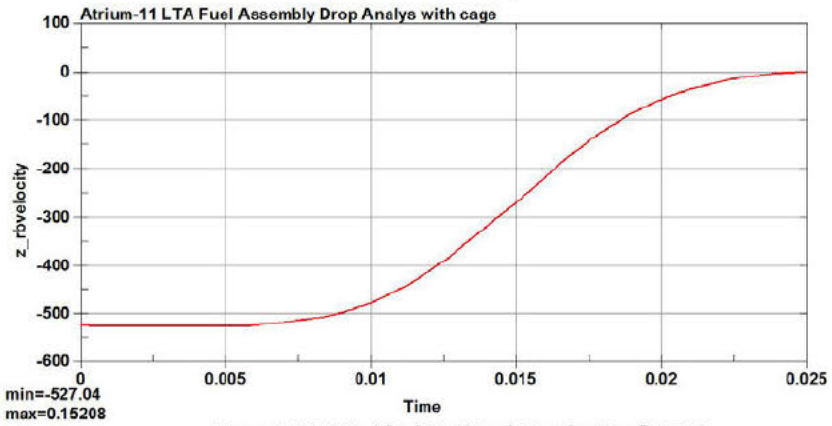

Figure C.6-4 Modified Rigid Body Z-velocity of Part 3

3. The modified acceleration curve is shown in Figure C.6-5 below. This is used as input to the single rod fuel model.

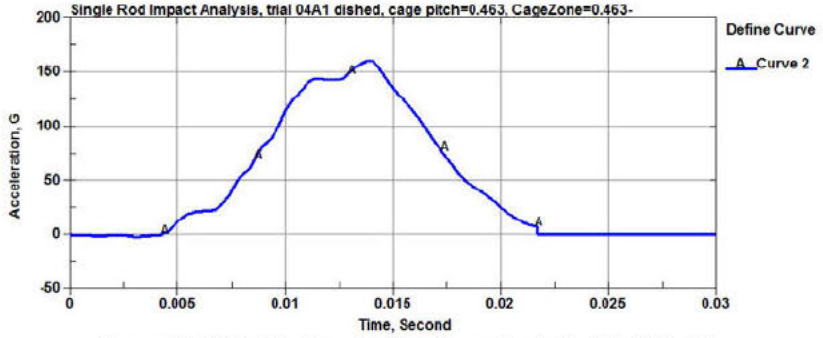

Figure C.6-5 Modified Acceleration Curve, Single Fuel Rod Model

Contact Definition.

[redacted]

The fuel pellets are free to move inside the fuel cladding tube. There is contact between the fuel cladding and the fuel pellets. The fuel pellets are also allowed to impact each other fuel pellets within the fuel cladding tube. So there is also contact between fuel pellets.

[redacted]

C.7 Pitch Change of Single Rod Fuel Model

The pitch change is the maximum absolute displacement change between two adjacent fuel rods. Since there is only one rod in the finite element model, the maximum permanent lateral displacement calculated from the LSDYNA analysis is half of the actual pitch change. The maximum lateral displacement in the XY-plane is shown in Figure C.7-1 below.

[redacted]

The predicted pitch change result reported by the single rod model is smaller than the average pitch change result reported in Tables C.4-1, but it is greater than the average pitch change result reported in Table C.4-2. However, the calculated pitch change from the single rod model is a single result that does not take into account an average of the statistical samples of the pitch change as calculated for the decoupled model with many fuel rods. The single rod result suggests that the lateral interaction between the fuel pellet and fuel cladding does not appear to be a significant effect, and that the predicted percent pitch changes are consistent between both finite element models.

C.8 Summary

From Section C.4, the decoupled bundled fuel model that considers all fuel rods through the section of the fuel rod assembly predicts an average pitch change is 2.6%. This value is smaller than the predicted pitch change of 4.8% from the single fuel rod model with a multiplication factor of ~two.

[redacted]

However, as discussed in Section C.2, the lateral deflections of individual fuel rods and the resulting pitch changes are phenomena best characterized by statistical methods, such as averaging.

From Section Table C.5-1, the average overall Outside Perimeter pitch change is 3.4%. This value is consistent with the averaged pitch changes calculated between the adjacent fuel rod pairs within the fuel bundle.

C.9 Description of Input Files

The input files for the analysis are described in this section and stored on the DVD. For each of the drop case, the folder name, file name, and the simple description of the file are listed.

Table C.9-1. LSDYNA Input Files, Fuel Bundles Model

Fuel Bundle Model		
Folder Name:	Input file name:	File Description
M:\AREVA Pin Pitch Task\Fuel Bundle Analysis	HAC014_FA1_480G_p1p2p3.k	A single file to start the analysis

Table C.9-2. LSDYNA Input Files, Single Rod Model

Folder Name:	Input file name:	File Description
M:\AREVA Pin Pitch Task\Single Rod Analysis	Single_Rod_run04C1.k	A file to start the analysis
	CLADDING_SURFACE.DYN	Cladding inside surface elements to apply pressure
	DISHED_ROD_NODES_ELEMENTS.dyn	Finite Element model of
	rim_nodes_top.dyn	Constraints applied to the nodes

C.10 Scripts Used To Post-Process the Fuel Bundle Drop Analysis

There are 2 post-processing script files that are used to assist extracting the results. They are described below.

File Name: **plot_Pitch_Changes.mac**
Purpose of Script File: For the selected node pairs, plot pitch change time histories and measure the absolute pitch changes. The outputs are plotted graphics and printed text files. The data is summarized in Tables C.4-1 and C.4-2

File Name: **plot_Bundle_OD_Changes.mac**
Purpose of Script File: For the selected node pairs, plot pitch change time histories and measure the absolute pitch changes. The outputs are plotted graphics and printed text files. The data is summarized in Table C.5-1